Brain, Behavior, & Immunity - Health 13 (2021) 100229

Contents lists available at ScienceDirect

Brain, Behavior, & Immunity - Health

journal homepage: www.editorialmanager.com/bbih/default.aspx

Full Length Article

Sex-specific responses of the pubertal neuroimmune axis in CD-1 mice

Daria Kolmogorova [a], Emily Grace Ah-Yen [a], Briallen Carys Taylor [b], Tiffany Vaggas [b], Jacky Liang [a], Tama Davis [a], Nafissa Ismail [a,c,*]

[a] NISE Laboratory, School of Psychology, University of Ottawa, Ottawa, Ontario, Canada
[b] School of Biosciences, Cardiff University, Cardiff, Wales, United Kingdom
[c] Brain and Mind Research Institute, University of Ottawa, Ottawa, Ontario, Canada

ARTICLE INFO

Keywords:
Lipopolysaccharide
Blood-brain barrier
Fractal analysis
Iba1
Caspase-3
NeuN

ABSTRACT

The mechanistic relationship between the sexually dimorphic neuroimmune system and the sex-specific outcomes of a pubertal immune challenge is unclear. Therefore, we examined sex differences in the progression of cytotoxic microglial responses and blood-brain barrier (BBB) disruption to a peripubertal lipopolysaccharide (LPS) treatment in brain regions relevant to stress responses and cognitive function. Six-week-old (i.e., stress-sensitive pubertal period) male and female CD-1 mice were treated with LPS (1.5 mg/kg body weight, *ip*) or 0.9% saline (LPS-matched volume, *ip*). Sex and treatment differences in microglial ($Iba1^+$) and apoptotic neuronal ($caspase\text{-}3^+/NeuN^+$) and non-neuronal ($caspase\text{-}3^+/NeuN^-$) expression were examined in the hippocampus, medial prefrontal cortex (mPFC), and paraventricular nucleus 24 h (sickness), one week (symptomatic recovery) and four weeks (early adulthood) post-treatment ($n = 8$/group). Microglial morphology was quantified with fractal analyses. Group differences in BBB permeability to ^{14}C-sucrose were examined 24 h (whole-brain, hippocampus, prefrontal cortex, hypothalamus, and cerebellum) and one week (whole-brain) post-treatment. The acute effects of pubertal LPS were specific to females (i.e., global BBB disruption, altered microglial expression and morphology in the mPFC and hippocampus, increased hippocampal apoptosis). The residual effects of pubertal LPS-induced sickness observed in microglia persisted into adulthood in a sex- and region-specific manner. In addition to highlighting these sex-specific responses of the pubertal neuroimmune system, we report baseline region-specific sex differences in microglia spanning puberty through adulthood. We propose that these sex differences in neuroimmune-neurovascular interactions during the stress-sensitive pubertal period create sex biases in stress-related disorders of brain and behaviour.

1. Introduction

Sex-specific patterning of the brain and the stress response system during puberty contribute to sex differences in stress vulnerability and reactivity during this critical period, particularly towards a systemic immune challenge (Holder and Blaustein, 2014; Kane and Ismail, 2017; Schulz and Sisk, 2016; Sisk and Foster, 2004; Vigil et al., 2011). Sex differences in the reorganization and remodelling of pubertal neurocircuitry facilitate the sex-specific outcomes of a pubertal immune challenge on brain and behaviour. For example, CD-1 mice treated with the bacterial endotoxin lipopolysaccharide (LPS) (1.5 mg/kg body weight, intraperitoneal [*ip*]) during the stress-sensitive pubertal period (i.e., six weeks of age) show female-skewed increases in depression-like behaviours and male-biased increases in anxiety-like behaviours and reactivity to novel stressors (Murray et al., 2019). Similar sex-dependent effects of pubertal LPS treatment are observed in stress and immune responses (Cai et al., 2016; Girard-Joyal et al., 2015; Sharma et al., 2019), behavioural responsiveness to gonadal hormones (Ismail et al., 2013; Laroche et al., 2009a,b; Olesen et al., 2011), spatial learning and hippocampal cell development (Kolmogorova et al., 2019), and dopamine-sensitive behaviours (Girard-Joyal and Ismail, 2017). The neural mechanisms driving the sex-specific acute and enduring effects of LPS treatment during the stress-sensitive pubertal period remain elusive.

The brain's primary line of immune defense is a system of microglia cells whose phagocytic properties lend themselves well to addressing immune threats (e.g., cellular debris, bacteria), shaping of neural circuits during critical periods, and maintaining neural networks (Lenz and Nelson, 2018; Li and Barres, 2018; Tay et al., 2017). Age-related sex differences in cell density and phenotype (e.g., Crain et al., 2013; Hanamsagar et al., 2017; Villa et al., 2018) establish region-dependent

* Corresponding author. 136 Jean-Jacques Lussier, Vanier Hall, Room 2076B, Ottawa, Ontario, K1N 6N5, Canada.
E-mail address: nafissa.ismail@uottawa.ca (N. Ismail).

https://doi.org/10.1016/j.bbih.2021.100229
Received 18 February 2021; Accepted 18 February 2021
Available online 24 February 2021

sexual dimorphisms in microglial functions. When faced with an immune threat, the highly ramified surveillant "resting" microglia alter their morphology along a graded continuum towards the amoeboid-like form of their fully "activated" phagocytic state (Hoogland et al., 2015). Intense systemic immune stressors can dysregulate adaptive microglia-mediated inflammatory responses (Ling et al., 2006; Puntener et al., 2012; Qin et al., 2007; Williamson et al., 2011). Maladaptive microglial responses generate excess cytotoxic factors (e.g., nitric oxide, tumour necrosis factor alpha) which activate programmed cell death pathways such as apoptosis (e.g., Cunningham et al., 2005; Khan et al., 2016; 2017; Noh et al., 2014). Due to genomic and hormonal influences, neonatal and young females adopt predominantly caspase-dependent apoptotic pathways during inflammatory events compared to the caspase-independent pathways more commonly seen among age-matched males (Alfonso--Loeches et al., 2013; Du et al., 2004; Liu et al., 2009; Rau et al., 2003; Waters and Simerly, 2009; Zhu et al., 2005, 2006).

As a key interface between the central nervous system (CNS) and the periphery, the blood-brain barrier (BBB) moderates neuroinflammatory responses to systemic immune events by restricting passage of peripheral immune-activating factors into the CNS (Abbott et al., 2006; Engelhardt and Liebner, 2014; Langen et al., 2019; Sweeney et al., 2019). High doses of systemic LPS (e.g., 3.0 mg/kg body weight) disrupt BBB integrity to small (^{14}C-sucrose [342 Da], sodium fluorescin [376 Da], ^{99m}Tc-DTPA [487 Da]) and large (^{13}I-albumin [66 kDa]) radioisotopes, with the most significant LPS-induced BBB disruption occurring 24 h post-treatment (Banks et al., 2015; Nishioku et al., 2009). The magnitude of regional and global BBB vulnerability to systemic immune events is influenced by age-related sex differences in circulating gonadal steroid hormones (Abi-Ghanem et al., 2020; Duckles and Krause, 2007; Erdö et al., 2016; Erickson and Banks, 2019; Krause et al., 2006). Although our understanding of the androgenic influences on the BBB is complicated by the natural conversion of androgens to estrogenic steroids in the body, androgens and progesterone appear to oppose the cerebrovascular effects of estrogens (Abi-Ghanem et al., 2020; Krause et al., 2002; Ospina et al., 2003; Robison et al., 2019). Androgens and progesterone generally constrict cerebrovascular tone and exert pro-inflammatory effects, whereas estrogens tend to dilate vascular tone, increase cerebral flow, and show immune-suppressing or anti-inflammatory properties (Gonzales et al., 2005, 2008; Krause et al., 2002; Ospina et al., 2003, 2004; Sunday et al., 2006).

This study tested the mechanistic involvement of the pubertal neuroimmune network in the sex-specific outcomes of systemic immune challenge during this critical period. We examined sex differences in the progression of LPS-induced effects on BBB permeability, microglial expression and morphology, and caspase-3-dependent apoptosis of neuronal and non-neuronal cells, focusing on the sexually dimorphic and interconnected brain regions for stress regulation and cognitive functioning. Acutely, systemic LPS treatment was expected to disrupt BBB integrity (i.e., whole brain and in the hippocampus, prefrontal cortex [PFC], hypothalamus, and cerebellum) and to induce apoptotic microglial responses in the hippocampus, medial PFC (mPFC), and paraventricular nucleus (PVN). LPS-induced BBB disruption and apoptosis were expected to subside upon symptomatic recovery, whereas the microglial changes were expected to persist into early adulthood. The magnitude of all LPS-induced effects was expected to differ betwen regions. Baseline sex differences in the pubertal neuroimmune network predict a generally female-biased vulnerability to LPS-induced changes in the examined systems.

2. Methods

2.1. Animals

Three-week-old male and female CD-1 mice were shipped to our animal facility from Charles River Laboratories (Saint-Constant, Québec). All mice were housed in groups of three in polycarbonate Lexan cages (17 × 28 × 12 cm [width x length x height]) in sex-segregated rooms maintained on a reversed light cycle (lights off at 1000 h) under standard conditions (14 h:10 h light/dark cycle; 24 ± 2 °C; relative humidity of 40 ± 5%). Dusk and dawn were induced gradually over 1 h. The cages included Teklad Corn Cob bedding (Harlan Laboratories, Inc., Madison, WI, USA; 0.25 in. diameter), a cardboard refuge hut (Ketchum Manufacturing, Inc., Brockville, ON, Canada), and one square piece of Nestlet (Ancare Corp., Bellmore, NY, USA). *Ad libitum* access to food (Harlan Laboratories, Inc., Madison, WI, US, T2018 – Global 18% rodent) and water was provided. The Animal Care Committee of the University of Ottawa approved all experimental procedures.

2.2. Treatment administration

Six-week-old mice received either LPS (from *Escherichia coli* serotype O26:B6; L#3755; Sigma Chemical Co., St. Louis, MO, USA; 1.5 mg/kg body weight, *ip*) or 0.9% sterile saline (LPS-matched volume, *ip*) towards the end of the light phase (n = 96/treatment). During puberty, this LPS dose induces sickness for approximately 48 h in both sexes and impairs stress- and cognition-related neurocircuitry and behaviour in a sex-dependent manner (Cai et al., 2016; Girard-Joyal et al., 2015; Kolmogorova et al., 2019; Sharma et al., 2019).

2.3. Sickness monitoring

Two experienced raters blinded to treatment examined each mouse 0.5, 2, 4, 8, 12, and 24 h post-treatment for behavioural signs of sickness (i.e., lethargy, piloerection, ptosis, and huddling). Scores between 0 and 4 were assigned to reflect the number of sickness behaviours observed (Kolmogorova et al., 2017). Mean scores at each time-point were used for analysis.

2.4. Body weight

Body weights were measured at time of injection (i.e., baseline) and 12 and 24 h post-treatment. Changes in body weight were examined as percent change in body weight from baseline (Kolmogorova et al., 2017).

2.5. Brain tissue collection

All mice were deeply anesthetized with sodium pentobarbital (500 mg/kg body weight, *ip*) at either 24 h, one week, or four weeks after LPS or saline exposure (n = 8/group). Upon confirmation of deep anesthesia, mice were intracardially perfused with sterile saline (20.0 mL) followed by 4% paraformaldehyde (PFA) (20.0 mL). The excised brains were post-fixed in 4% PFA for 2 h and then placed in fresh 30% sucrose solution 2 and 24 h after post-fixing. The brain tissue was sliced by vibratome into 30 μm free-floating sections into four equal series and stored in cryoprotectant solution at −20 °C.

2.6. Immunohistofluorescence for Iba1

Staining for microglia was completed on one series of brain tissue. All steps were performed at room temperature with gentle agitation, unless otherwise specified. Free-floating sections were first washed in 0.3% TritonX-100/1X phosphate-buffered saline (PBS; three x 5 min). After 2 h blocking with a 1% bovine serum albumin (BSA)/ 0.3% TritonX-100/1X PBS solution, the tissue was incubated for 24 h at 4 °C in a solution of rabbit anti-Iba1 (1:1000; Wako Laboratory Chemicals; cat: 019–19741)/ 1% BSA/ 0.3% TritonX-100/1X PBS. The sections were again rinsed in 0.3% TritonX-100/1X PBS (three x 5 min) and then incubated with Alexa Fluor® 488 (1/2000; ThermoFisher Scientific; cat: A21206) in a 1% BSA/ 0.3% TritonX-100/1X PBS solution for 2 h. A final set of washes in 0.3% TritonX-100/1X PBS (three x 5 min) was completed before mounting onto glass slides using DPX mountant (Sigma-Aldrich; cat: 06522) and coverslip.

2.7. Double-labelling for Caspase-3 and NeuN

A second series of brain tissue was used to double-label for neurons (i.e., NeuN) and apoptotic cells (cleaved caspase-3). Caspase-3 is a key executioner of programmed cell death in both the mitochondrial (intrinsic) and death receptor (extrinsic) pathways of apoptosis (Elmore, 2007; Shalini et al., 2015). The procedures were performed at room temperature with gentle agitation, unless otherwise specified. Briefly, the tissue was rinsed in 0.3% Triton X-100/1X PBS (three x 5 min) and then blocked with 1% donkey serum/ 0.3% TritonX-100/1X PBS for 2 h. NeuN and caspase-3 labelling was achieved with guinea pig anti-NeuN (1/2000; Millipore; cat: ABNP) and rabbit anti-caspase-3 (1/1000; Cell Signaling Technologies; cat: 9661) diluted in 1% donkey serum/ .3% TritonX-100/1X PBS (24 h incubation at 4 °C). Following a second wash (0.3% TritonX-100/1X PBS; three x 5 min), the staining was visualized using donkey anti-guinea pig Alexa Fluor® 488 (1/1000; Jackson Immuno Research; cat: 706-545-148) and donkey anti-rabbit Alexa Fluor® 594 (1/2000; Life Technology; cat: A21207) diluted in 1% donkey serum/ 0.3% TritonX-100/1X PBS (2 h incubation). The tissue was again washed in 0.3% TritonX-100/1X PBS (three x 5 min). Nuclear counterstaining was achieved by immersing the tissue in Hoechst 33342 (1/20,000; Invitrogen; cat: H3570)/1X PBS for 10 min. After a final set of

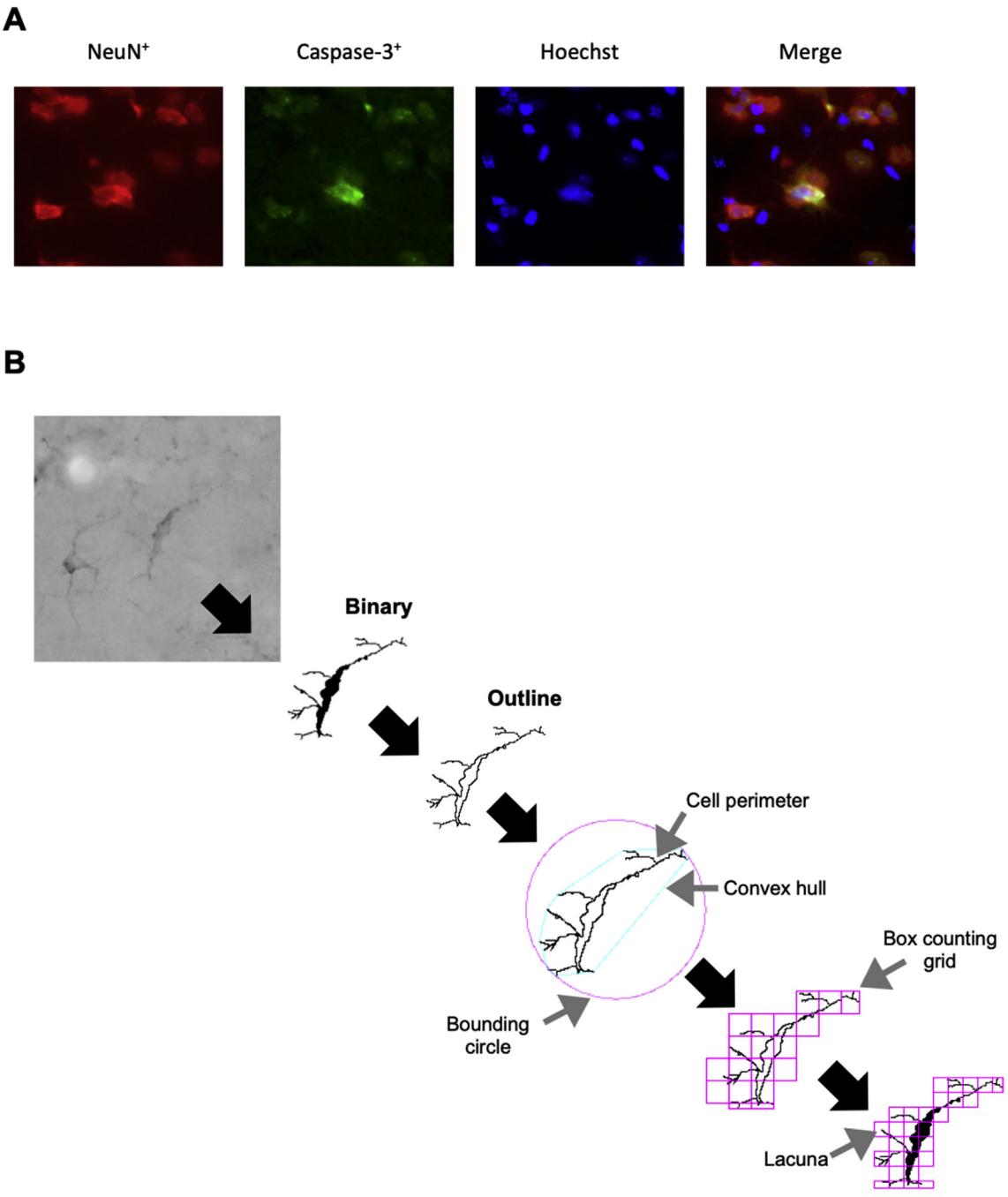

Fig. 1. *Apoptotic cells and morphometric analyses of microglial cells.*
Note. Caspase-3^{+}/NeuN^{+} cells (i.e., apoptotic neurons) showed identical co-labelling with Hoechst (**A**). Caspase-3^{+} cells without this colocalization of Hoechst with nearby NeuN^{+} cells were considered non-neuronal (i.e., caspase-3^{+}/NeuN^{-} cells). To analyze morphometric features of the randomly selected Iba1^{+} cells, the original photomicrographs were made binary and then converted to outlines in Fiji for fractal analyses using the FracLac plugin (**B**) (Karperien et al., 1999–2013; Morrison et al., 2017).

washes (0.3% TritonX-100/1X PBS; three x 5 min), the tissue was mounted onto glass slides using with DPX mountant (Sigma-Aldrich; cat: 06522) and coverslip.

2.8. Cell quantification

Quantification of Iba1$^+$, caspase-3$^+$, caspase-3$^+$/NeuN$^-$, and caspase-3$^+$/NeuN$^+$ cells in the hippocampus, hippocampal sub-regions (i.e., dentate gyrus [DG], cornus ammonis [CA]1, CA2, and CA3), mPFC, and PVN was assessed by averaging the total cell counts of two trained raters blinded to experimental group. Cell quantification was completed on one representative bilateral image of the dorsal hippocampus (i.e., bregma: −2.18 mm), mPFC (i.e., bregma: +1.78 mm), and the PVN (i.e., bregma: −0.82 mm) (Franklin and Paxinos, 2007). All images were captured using a 20× objective on an Olympus BX61 microscope. Iba1$^+$ cells were counted only when a cell body was clearly identifiable. Colocalization with Hoechst was required for counting both caspase-3$^+$ and NeuN$^+$ cells. Caspase-3$^+$/NeuN$^+$ cells showed identical Hoechst co-labelling (see Fig. 1A).

2.9. Quantitative analyses of microglial morphology

Fractal analyses were performed using Fiji software (Schindelin et al., 2012). Iba1$^+$ cells for fractal analysis were randomly selected using a grid and random number generator (n = 24 cells/bilateral region) (Morrison et al., 2017). Photomicrographs of selected Iba1$^+$ cells were first made binary and then converted to outlines in Fiji (Karperien et al., 1999–2013; Morrison et al., 2017) (see Fig. 1B). The FracLac plugin (Karperien, 1999–2013) was then applied to the outline of each microglia cell to quantify density, fractal dimension (using a box plot protocol), lacunarity (using a box plot protocol), span ratio, and cell circularity (see Table 1).

2.10. Radioactive measures of in vivo BBB disruption

In vivo BBB disruption was assessed at 24 h (whole-brain and region) and at one week (whole-brain) after saline or LPS treatment (n = 8/group). In brief, mice were deeply anesthetized with 0.1–0.2 mL of 40% urethane (*ip*) and then injected with ^{14}C-sucrose (10^6 *dpm* in 0.2 mL of lactated Ringer's solution/1% BSA) into the jugular vein (Banks et al., 2015). After 10 min, arterial blood was collected from the descending abdominal aorta, the descending thoracic aorta was clamped, the left and right jugular veins were severed, and 20.0 mL of lactated Ringer's solution was perfused through the left heart ventricle in under 1 min. Whole brains and hippocampal, PFC, cerebellar, or hypothalamic tissue were then excised, weighed, and solubilized. Serum was obtained by centrifuging the collected blood for 5 min at 10,000×*g*. Total levels of radioactivity in the brain and serum were measured using a PerkinElmer Tri-Carb 2910 TR scintillation counter. Data are expressed as mean counts per minute (CPM) per brain sample (g) divided by the CPM per μL in the corresponding serum (μL/g).

2.11. Experimental procedures

Male and female CD-1 mice were treated with LPS or saline at six weeks of age, a stress-sensitive period during puberty (Laroche et al., 2009a,b). A subset of mice was used for immunohistofluorescence to assess sex and treatment differences in microglial expression and morphology and caspase-3-dependent apoptosis of neuronal and non-neuronal cells in the hippocampus, mPFC, and PVN over time (i.e., 24 h [sickness], one week [symptomatic recovery], and four weeks post-treatment [early adulthood]). Sex- and treatment-dependent changes in BBB disruption during sickness and symptomatic recovery were examined in the remaining mice. BBB disruption during sickness was examined in the whole-brain and regionally in the hippocampus, PFC, cerebellum, and hypothalamus; whole-brain BBB disruption was examined during symptomatic recovery. Sample sizes were consistent across all parameters (n = 8/experimental group).

2.12. Statistical analyses

Extreme statistical outliers (i.e., cases that exceed the 3 x interquartile range in boxplots) were adjusted by winsorization. Sex (male versus female) and treatment (saline versus LPS) effects on sickness parameters over time were examined with a three-way mixed-design analysis of variance (ANOVA) (Kolmogorova et al., 2017). The Greenhouse-Geisser correction was applied to F-values that violated Mauchly's test of sphericity (i.e., $\varepsilon_{\text{Greenhouse-Geisser}} < 0.75$). The expression of Iba1$^+$, caspase-3$^+$, caspase-3$^+$/NeuN$^-$, and caspase-3$^+$/NeuN$^+$ cells, and the morphometric profiles of Iba1$^+$cells, and ^{14}C-sucrose whole-brain/serum ratios were analyzed using a three-way (time x sex x treatment) between-subjects ANOVA. ^{14}C-sucrose whole-brain/serum ratios for hippocampal, PFC, hypothalamic, and cerebellar tissue were analyzed with a two-way (sex x treatment) between-subjects ANOVA. Statistical significance was set to $p < .05$. To protect from Type I error, Bonferroni correction was applied to *post hoc* pairwise comparisons of statistically significant interactions (Abdi, 2007). Trending interactions (i.e., $.05 < p < .10$) are only reported when corresponding Bonferroni-corrected pairwise comparisons were statistically significant. Effect sizes were estimated using partial eta-squared (η_p^2). All analyses were completed with IBM® SPSS® (version 20.0.0) statistical software.

3. Results

3.1. Acute behavioural and physical responses to treatment

The ANOVA of sickness behaviours showed a significant time x sex × treatment interaction ($F_{(3.85,\ 724.68)} = 2.45$, $p = .047$, $\eta_p^2 = 0.013$) (see

Table 1
Morphometric measures of microglia cells.

Dimension	Measure	Unit	Interpretation	Range
Fractal dimension	$\frac{\ln N\varepsilon}{\ln \varepsilon}$	D_B	Measure of cell's contour bounded by endpoints and process lengths	1–2
Circularity	$\frac{4\pi \text{ x cell area}}{\text{cell perimeter}^2}$	Ratio	Roundness	0–1
Span ratio	$\frac{\textit{convex hull eclipse longest length}}{\textit{convex hull eclipse longest width}}$	Ratio	Cell shape	0–1
Lacunarity	$\frac{\Sigma\Lambda_{(g)}}{N_{(G)}}$	λ	Distribution of gaps or lacuna in the image	>0
Density	$\frac{\#\text{ of pixels within cell outline}}{\text{area of convex hull}}$	$\frac{\#\text{ of pixels}}{\text{area}}$	Cell size	0–1

Note. N refers to the number of pixels; ε refers to box size or scale; $N_{(G)}$ refers to the number of grid origins; $\Lambda_{(g)}$ refers to the calculated mean lacunarity (λ) per image (Karperien et al., 2013).

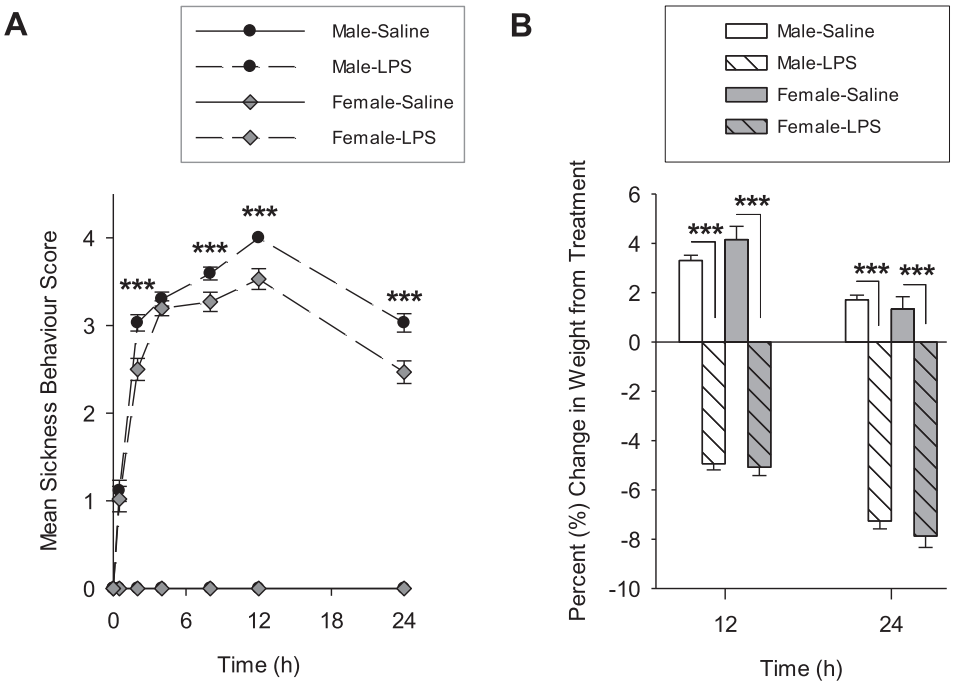

Fig. 2. Mean sickness scores and changes in body weight of six-week-old male and female CD-1 mice following treatment.
Note. Sickness behaviours were examined.5, 2, 4, 8, 12, and 24 h after treatment with LPS (1.5 mg/kg body weight, *ip*) or 0.9% sterile saline (LPS-matched volume, *ip*). Body weights were measured at time of treatment and 12 and 24 h post-treatment to examine percent change in body weight from time of treatment. Data presented as mean (±*SEM*) sickness scores (**A**) and percent (%) change in body weight (**B**). Asterisks denote significant sex differences (**A**) and treatment differences (**B**) (* = $p < .05$, ** = $p < .01$, *** = $p < .001$).

Fig. 2A). As expected, sickness behaviour responses changed significantly over the 24 h observation period ($F_{(3.85,\ 724.68)} = 202.47$, $p < .001$, $\eta_p^2 = 0.519$) and were consistently higher among LPS-treated mice compared to their saline-treated counterparts ($F_{(1,\ 188)} = 4427.20$, $p < .001$, $\eta_p^2 = 0.959$). Sickness behaviour responses were also significantly affected by sex ($F_{(1,\ 188)} = 16.56$, $p < .001$, $\eta_p^2 = 0.081$). Among LPS-treated mice, males and females showed similar increases in sickness behaviours 30 min post-treatment; however, mean sickness behaviour responses were significantly higher among LPS-treated males relative to their female counterparts at 2, 8, 12, and 24 h post-treatment (mean difference [*MD*] = 0.53, standard error [*SE*] = 0.11; *MD* = 0.32, *SE* = 0.09; *MD* = 0.47, *SE* = 0.08; and *MD* = 0.56, *SE* = 0.12, respectively; all $p \leq .001$).

Analyses of percent change in body weight from baseline revealed a significant time × treatment interaction ($F_{(2,\ 376)} = 1273.13$, $p < .001$, $\eta_p^2 = 0.684$) and significant main effects of time ($F_{(2,\ 376)} = 155.37$, $p < .001$, $\eta_p^2 = 0.452$) and treatment ($F_{(1,\ 188)} = 728.74$, $p < .001$, $\eta_p^2 = 0.795$) (see Fig. 2B). Baseline body weight did not differ between saline- and LPS-treated mice ($p > .05$). LPS treatment induced significant body weight loss in both male and female mice than their saline-treated counterparts 12 h and 24 h post-treatment (all $p < .001$). Males and females showed similar treatment-related percent changes in body weight (all $p > .05$).

3.2. Treatment and sex differences in hippocampal microglial expression

3.2.1. Total

Hippocampal microglia expression revealed a significant time × sex interaction ($F_{(2,\ 84)} = 3.15$, $p = .048$, $\eta_p^2 = 0.070$), as well as significant main effects of treatment ($F_{(1,\ 84)} = 5.43$, $p = .022$, $\eta_p^2 = 0.061$) and sex ($F_{(1,\ 84)} = 6.07$, $p = .016$, $\eta_p^2 = 0.067$) (see Fig. 3B). Saline-treated males expressed more Iba1$^+$ cells in the hippocampus than their female counterparts at both 24 h and one week post-treatment (*MD* = 357.75, *SE* = 123.94, $p = .005$ and *MD* = 302.63, *SE* = 123.94, $p = .017$, respectively). LPS-treated females showed significantly more total Iba1$^+$ cells than saline-treated females during symptomatic recovery (*MD* = 342.06, *SE* = 123.94, $p = .007$). Microglial expression in the hippocampus was similar across groups during adulthood (all $p > .05$).

3.2.2. DG

DG expression of microglia showed significant time x sex ($F_{(2,\ 84)} = 3.19$, $p = .046$, $\eta_p^2 = 0.071$) and sex x treatment ($F_{(1,\ 84)} = 5.22$, $p = .025$, $\eta_p^2 = 0.058$) interactions, as well as significant main effects of treatment ($F_{(1,\ 84)} = 4.01$, $p = .049$, $\eta_p^2 = 0.046$) and sex ($F_{(1,\ 84)} = 8.42$, $p = .005$, $\eta_p^2 = 0.091$) (see Fig. 4A). Iba1$^+$ cell counts in the DG were significantly higher 24 h and one week post-treatment among saline-treated males relative to saline-treated females (*MD* = 161.69, *SE* = 49.15, $p = .001$ and *MD* = 137.63, *SE* = 49.15, $p = .006$, respectively). At one week post-treatment, Iba1$^+$ cell counts were significantly higher among LPS-treated females relative to saline-treated females (*MD* = 128.69, *SE* = 49.15, $p = .010$). Microglial expression in the DG during adulthood was similar across groups (all $p > .05$).

3.2.3. CA1

Microglial expression in the CA1 revealed a significant time × sex interaction ($F_{(2,\ 84)} = 3.87$, $p = .025$, $\eta_p^2 = 0.084$) and significant main effects of treatment ($F_{(1,\ 84)} = 5.95$, $p = .017$, $\eta_p^2 = 0.066$) and sex ($F_{(1,\ 84)} = 8.81$, $p = .004$, $\eta_p^2 = 0.095$) (see Fig. 4B). Saline-treated males expressed more Iba1$^+$ cells in the CA1 than saline-treated females 24 h and one week post-treatment (*MD* = 126.75, *SE* = 45.39, $p = .006$ and *MD* = 124.82, *SE* = 45.39, $p = .007$, respectively). LPS-treated females expressed more Iba1$^+$ cells in the CA1 than their saline-treated counterparts one week post-treatment (*MD* = 105.63, *SE* = 45.39, $p = .022$). Microglial expression in the CA1 was similar across groups during adulthood (all $p > .05$).

3.2.4. CA2

Microglial expression in the CA2 was similar across groups at each time-point (all $p > .05$) (see Fig. 4C).

3.2.5. CA3

Microglial expression in the CA3 differed significantly across time ($F_{(2,\ 84)} = 5.26$, $p = .007$, $\eta_p^2 = 0.111$) (see Fig. 4D). Although the interactions were not statistically significant (all $p > .05$), the time-point x sex × treatment interaction was trending towards significance ($F_{(2,\ 84)} =$

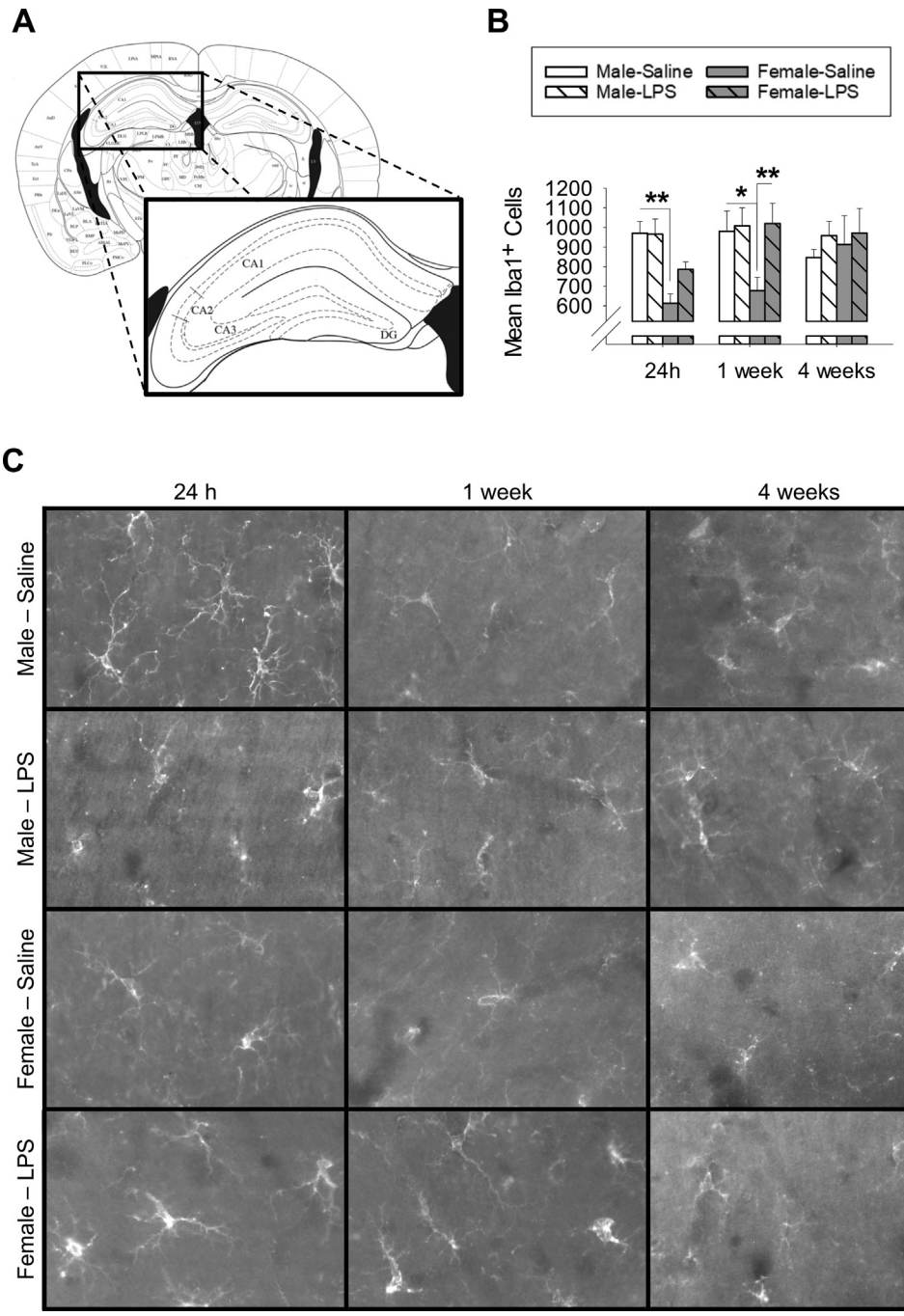

Fig. 3. Microglial expression in the hippocampus.
Note. Schematic drawing depicting the region of interest in the dorsal hippocampus and its subregions (i.e., bregma: −2.18 mm) (Franklin and Paxinos, 2007) (**A**). Data presented as mean (±*SEM*) total Iba1$^+$ cells counted in the whole hippocampus (**B**). Photomicrographs of hippocampal Iba1$^+$ cells from the experimental groups from the three time-points (i.e., 24 h, one week, and four weeks post-treatment) (**C**). Asterisks depict significant sex and treatment differences (* = $p < .05$, ** = $p < .01$, *** = $p < .001$).

2.79, $p = .067$, $\eta_p^2 = 0.067$). Microglial expression in the CA3 was similar across groups 24 h post-treatment (all $p > .05$). Iba1$^+$ cell expression was significantly higher one week post-treatment among LPS-treated females relative to saline-treated females (*MD* = 72.25, *SE* = 32.88, $p = .031$). During adulthood, LPS-treated males had significantly higher Iba1$^+$ cell counts relative to their saline-treated counterparts (*MD* = 66.50, *SE* = 32.88, $p = .046$).

3.3. Morphometric features of hippocampal microglia

Analyses of microglial morphology in the hippocampus (see Fig. 5A–E) revealed a significant time × sex interaction for density ($F_{(2, 84)} = 4.10$, $p = .020$, $\eta_p^2 = 0.089$) and a significant sex × treatment interaction for D_B ($F_{(1, 84)} = 5.90$, $p = .017$, $\eta_p^2 = 0.066$). Trends towards statistical significance were observed for the time × sex interaction for span ratio ($F_{(2, 84)} = 3.04$, $p = .053$, $\eta_p^2 = 0.068$) and the sex × treatment interaction for lacunarity ($F_{(1, 84)} = 3.41$, $p = .068$, $\eta_p^2 = 0.039$). D_B values differed significantly across time ($F_{(2, 84)} = 3.41$, $p = .038$, $\eta_p^2 = 0.075$). A significant main effect of treatment was observed for density ($F_{(1, 84)} = 8.38$, $p = .005$, $\eta_p^2 = 0.091$) and D_B ($F_{(1, 84)} = 10.91$, $p = .001$, $\eta_p^2 = 0.115$), as well as a significant main effect of sex for density ($F_{(1, 84)} = 11.44$, $p = .001$, $\eta_p^2 = 0.120$). Hippocampal microglia of LPS-treated mice consistently showed significantly higher circularity and lacunarity compared to those of saline-treated controls ($F_{(1, 84)} = 8.78$, $p = .004$, $\eta_p^2 = 0.095$ and $F_{(1, 84)} = 5.00$, $p = .028$, $\eta_p^2 = 0.056$, respectively). Span ratios were significantly lower among LPS-treated mice relative to controls ($F_{(1, 84)} = 16.13$, $p < .001$, $\eta_p^2 = 0.161$).

During LPS-induced sickness, hippocampal microglia showed significantly higher D_B values among LPS-treated females relative to saline-treated females (*MD* = 0.05, *SE* = 0.02, $p = .005$). One week post-treatment, density

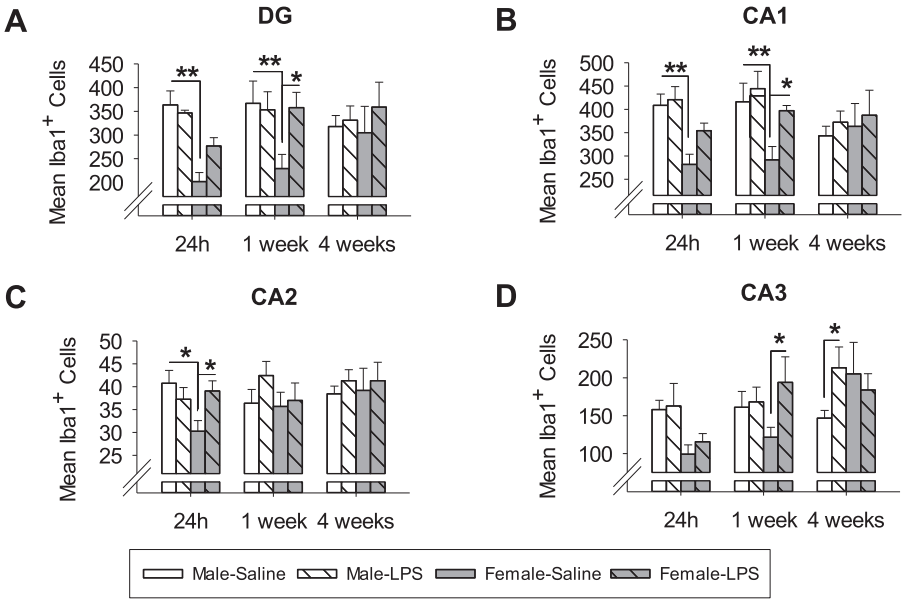

Fig. 4. Microglial expression in the hippocampal subregions.
Note. Mean (±*SEM*) total Iba1^{+} cells counted in dentate gyrus (**A**), cornus ammonis (CA) 1 (**B**), CA2 (**C**), and CA3 (**D**) 24 h, one week, and four weeks post-treatment. Asterisks depict significant sex and treatment differences (* = $p < .05$, ** = $p < .01$, *** = $p < .001$).

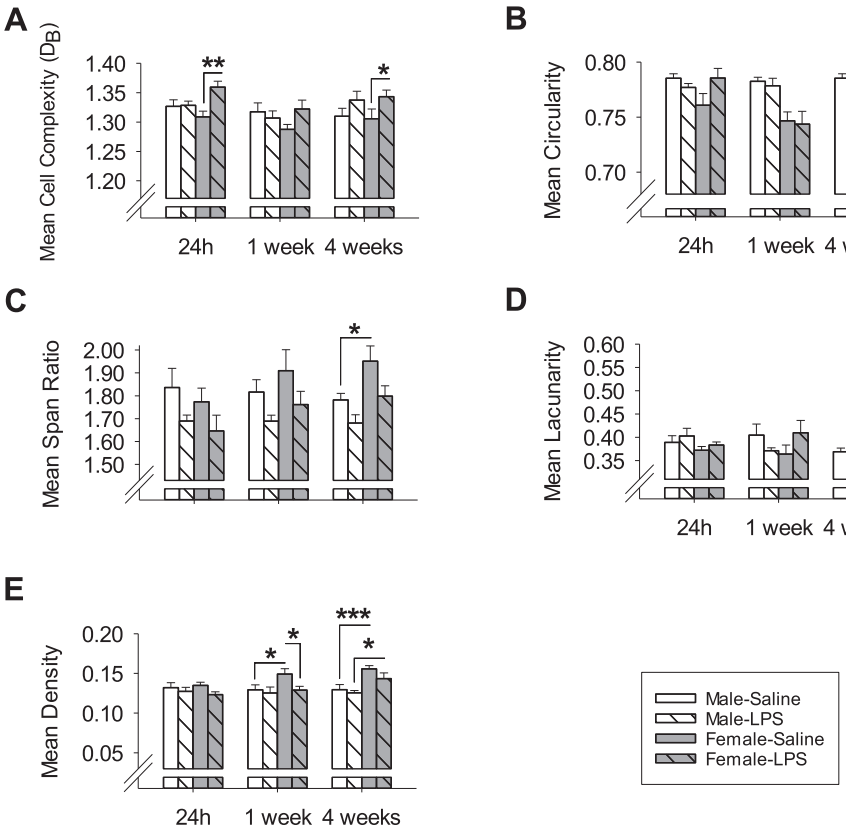

Fig. 5. Sex and treatment differences in microglial morphology in the hippocampus.
Note. The figures depict group means (±*SEM*) in fractal analyses (i.e., fractal dimension [**A**], circularity [**B**], span ratio [**C**], lacunarity [**D**], and density [**E**]) of hippocampal microglia 24 h, one week, and four weeks post-treatment. Asterisks denote significant sex and treatment differences (* = $p < .05$, ** = $p < .01$, *** = $p < .001$).

was significantly higher among saline-treated females relative to their LPS-treated counterparts ($MD = 0.02$, $SE = 0.01$, $p = .014$) and saline-treated males ($MD = 0.02$, $SE = 0.01$, $p = .015$). Hippocampal microglia four weeks post-treatment showed significantly greater lacunarity and density among LPS-treated females compared to saline-treated females ($MD = 0.07$, $SE = 0.03$, $p = .008$ and $MD = 0.03$, $SE = 0.01$, $p = .001$, respectively) and LPS-treated males ($MD = 0.05$, $SE = 0.03$, $p = .042$ and $MD = 0.02$, $SE = 0.01$, $p = .028$, respectively). Microglial span ratios were significantly higher in saline-treated females relative to male counterparts during adulthood ($MD = 0.17$, $SE = 0.08$, $p = .041$).

3.4. Hippocampal apoptosis

Hippocampal caspase-3-dependent apoptosis showed a significant time x sex × treatment interaction ($F_{(2, 84)} = 15.50, p < .001, \eta_p^2 = 0.270$) and significant main effects of time ($F_{(2, 84)} = 9.93, p < .001, \eta_p^2 = 0.191$), sex ($F_{(1, 84)} = 7.14, p = .009, \eta_p^2 = 0.078$), and treatment ($F_{(1, 84)} = 18.29, p < .001, \eta_p^2 = 0.179$) (see Table 2). Mean hippocampal caspase-3$^+$ cell expression 24 h post-treatment was significantly higher among LPS-treated females relative to saline-treated females ($MD = 3.25$, $SE = 0.38$, $p < .001$) and LPS-treated males ($MD = 3.25$, $SE = 0.38$, $p < .001$). Significant sex and treatment differences were not observed at later time-points (all $p > .05$).

3.4.1. Neuronal and non-neuronal apoptosis

Analyses of hippocampal apoptosis also revealed significant time x sex × treatment interactions for apoptosis of neuronal (i.e., caspase-3$^+$/NeuN$^+$) ($F_{(2, 84)} = 9.30, p < .001, \eta_p^2 = 0.181$) and non-neuronal (i.e., caspase-3$^+$/NeuN$^-$) cells ($F_{(2, 84)} = 5.73, p = .005, \eta_p^2 = 0.120$) (see Table 2). Significant main effects of time, sex, and treatment were observed for neuronal ($F_{(2, 84)} = 7.14, p = .001, \eta_p^2 = 0.145$; $F_{(1, 84)} = 6.07, p = .016, \eta_p^2 = 0.067$; and $F_{(1, 84)} = 10.37, p = .002, \eta_p^2 = 0.110$, respectively) and non-neuronal cells ($F_{(2, 84)} = 5.73, p = .005, \eta_p^2 = 0.120$; $F_{(1, 84)} = 5.73, p = .019, \eta_p^2 = 0.064$; and $F_{(1, 84)} = 5.73, p = .019, \eta_p^2 = 0.064$, respectively). At 24 h post-treatment, LPS-treated females had significantly more caspase-3$^+$/NeuN$^+$ and caspase-3$^+$/NeuN$^-$ cells than saline-treated females ($MD = 1.88$, SE = 0.27, $p < .001$ and $MD = 0.75$, $SE = 0.13$, $p < .001$, respectively) and LPS-treated males ($MD = 1.88$, SE = 0.27, $p < .001$ and $MD = 0.75$, $SE = 0.13$, $p < .001$, respectively). Neuronal and non-neuronal apoptosis was similar across groups one week and four weeks post-treatment (all $p > .05$).

3.5. Temporal sex and treatment effects on total microglial expression in the mPFC

Microglial expression in the mPFC revealed a significant time × sex interaction ($F_{(2, 84)} = 5.22, p = .007, \eta_p^2 = 0.110$) and a significant main effect of sex ($F_{(1, 84)} = 10.43, p = .002, \eta_p^2 = 0.110$) (see Fig. 6B). Iba1$^+$ cell numbers in the mPFC did not differ between groups 24 h and one week post-treatment (all $p > .05$). Four weeks post-treatment, however, mean Iba$^+$ cell counts were significantly higher among males relative to females in saline-treated and LPS-treated mice ($MD = 171.19$, $SE = 56.66$, $p = .003$ and $MD = 188.56$, $SE = 56.66$, $p = .001$).

Table 2
Caspase-3-dependent apoptosis in the hippocampus.

Cell	Time post-treatment	Males		Females	
		Saline-treated	LPS-treated	Saline-treated	LPS-treated
Caspase-3$^+$	24 h	.00 (.00)	.0 (.00)	.0 (.00)	3.25 (.80)
	1 week	.00 (.00)	.00 (.00)	.00 (.00)	.00 (.00)
	4 weeks	.00 (.00)	.75 (.49)	.00 (.00)	.00 (.00)
Caspase-3$^+$/ NeuN$^+$	24 h	.00 (.00)	.0 (.00)	.0 (.00)	1.88 (.64)
	1 week	.00 (.00)	.00 (.00)	.00 (.00)	.00 (.00)
	4 weeks	.00 (.00)	.25 (.16)	.00 (.00)	.00 (.00)
Caspase-3$^+$/ NeuN$^-$	24 h	.00 (.00)	.00 (.00)	.0 (.00)	.75 (.31)
	1 week	.00 (.00)	.00 (.00)	.00 (.00)	.00 (.00)
	4 weeks	.00 (.00)	.00 (.00)	.00 (.00)	.00 (.00)

Note. Data present group means (±*SEM*) of total caspase-3$^+$, caspase-3$^+$/NeuN$^+$ (i.e., neuronal), and caspase-3$^+$/NeuN$^-$ (i.e., non-neuronal) cells counted in the hippocampus. Asterisks denote significant sex and treatment differences (* = $p <$ .05, ** = $p < .01$, *** = $p < .001$).

3.6. Morphometric features of microglia in the mPFC

Fractal analyses in the mPFC (see Fig. 7A–E) identified significant time x sex ($F_{(2, 84)} = 3.16$, $p = .048$, $\eta_p^2 = 0.070$) and time x sex × treatment interactions ($F_{(2, 84)} = 3.51$, $p = .034$, $\eta_p^2 = 0.077$) for circularity. There were trends towards statistical significance for the time × treatment interaction for span ratio ($F_{(2, 84)} = 2.94, p = .059, \eta_p^2 = 0.065$) and the time x sex × treatment interaction for D_B values ($F_{(2, 84)} = 2.55, p = .084, \eta_p^2 = 0.057$). Circularity, D_B, and span ratios varied significantly across time ($F_{(2, 84)} = 4.30, p = .017, \eta_p^2 = 0.093$; $F_{(2, 84)} = 3.32, p = .041, \eta_p^2 = 0.073$; and $F_{(2, 84)} = 6.94$, $p = .002$, $\eta_p^2 = 0.142$, respectively). A significant main effect of sex was observed for circularity ($F_{(1, 84)} = 22.85, p < .001, \eta_p^2 = 0.214$). Span ratios and density values were overall significantly higher among females compared to males ($F_{(1, 84)} = 16.13$, $p < .001$, $\eta_p^2 = 0.161$ and $F_{(1, 84)} = 23.40, p < .001, \eta_p^2 = 0.218$, respectively). In contrast, D_B and lacunarity values were significantly skewed towards males ($F_{(1, 84)} = 22.81, p < .001, \eta_p^2 = 0.214$ and $F_{(1, 84)} = 42.90$, $p < .001$, $\eta_p^2 = 0.338$, respectively).

Microglia in the mPFC 24 h post-treatment showed significantly higher span ratios among saline-treated females relative to LPS-treated females ($MD = 0.15$, $SE = 0.05$, $p = .006$) and saline-treated males ($MD = 0.14$, $SE = 0.05$, $p = .012$). Female controls also showed significantly lower D_B values than saline-treated males ($MD = -0.04$, $SE = 0.02$, $p = .025$) and less circularity than LPS-treated females ($MD = -0.03$, $SE = 0.01$, $p = .027$) and saline-treated males ($MD = -0.02$, $SE = 0.01$, $p = .028$) at this time-point. One week post-treatment, D_B values, lacunarity, circularity were significantly skewed towards males in saline-treated ($MD = 0.04$, $SE = 0.02$, $p = .045$; $MD = 0.04$, $SE = 0.02$, $p = .015$ and $MD = 0.04$, $SE = 0.01$, $p = .001$, respectively) and LPS-treated mice ($MD = 0.08$, $SE = 02$, $p < .001$; $MD = 0.08$, $SE = 0.02$, $p < .001$; and $MD = 0.04$, $SE = 0.01$, $p = .002$, respectively). Conversely, span ratios one week post-treatment were significantly greater among females relative to males in saline-treated and LPS-treated mice ($MD = 0.19$, $SE = 0.05$, $p = .001$) and LPS-treated mice ($MD = 0.16$, $SE = 0.05$, $p = .003$). This female bias in span ratios among saline-treated and LPS-treated mice persisted into adulthood ($MD = 0.11$, $SE = 0.05$, $p = .039$ and $MD = 0.13$, $SE = 0.05$, $p = .014$, respectively). LPS-treated females displayed significantly less circularity in microglia than females ($MD = -0.02$, $SE = 0.01$, $p = .045$) and LPS-treated males ($MD = -0.03$, $SE = 0.01$, $p = .003$) four weeks post-treatment. D_B and lacunarity values during adulthood were significantly higher among LPS-treated males relative to LPS-treated females ($MD = 0.04$, $SE = 0.02$, $p = .049$ and $MD = 0.05$, $SE = 0.02$, $p = .003$, respectively). The microglia of adult male controls showed significantly greater lacunarity than their female counterparts ($MD = 0.04$, $SE = 0.02$, $p = .029$).

3.7. Apoptosis in the mPFC

Caspase-3 activity in the mPFC showed significant interactions of time x treatment ($F_{(2, 84)} = 3.18, p = .047, \eta_p^2 = 0.070$) and time x sex x treatment ($F_{(2, 84)} = 3.18, p = .047, \eta_p^2 = 0.070$) and a significant main effect of sex ($F_{(1, 84)} = 6.24, p = .014, \eta_p^2 = 0.069$) (see Table 3). Mean caspase-3$^+$ cell numbers were similar across groups 24 h and one week post-treatment (all $p > .05$). During adulthood, however, LPS-treated males had significantly higher mean capase-3$^+$ cell expression compared to saline-treated males ($MD = 0.38$, $SE = 0.14$, $p = .010$) and LPS-treated females ($MD = 0.38$, $SE = 0.14$, $p = .010$).

3.7.1. Neuronal and non-neuronal apoptosis

Among apoptotic cells in the mPFC, neuronal cells showed significant interactions of time x treatment ($F_{(2, 84)} = 3.18, p = .047, \eta_p^2 = 0.070$) and time x sex x treatment ($F_{(2, 84)} = 3.18, p = .047, \eta_p^2 = 0.070$) and a significant main effect of sex ($F_{(1, 84)} = 6.24, p = .014, \eta_p^2 = 0.069$) (see Table 3). Neuronal apoptosis in the mPFC was similar across groups 24 h and one week post-treatment (all $p > .05$). Caspase-3$^+$/NeuN$^+$ cell expression during adulthood was significantly higher among LPS-treated

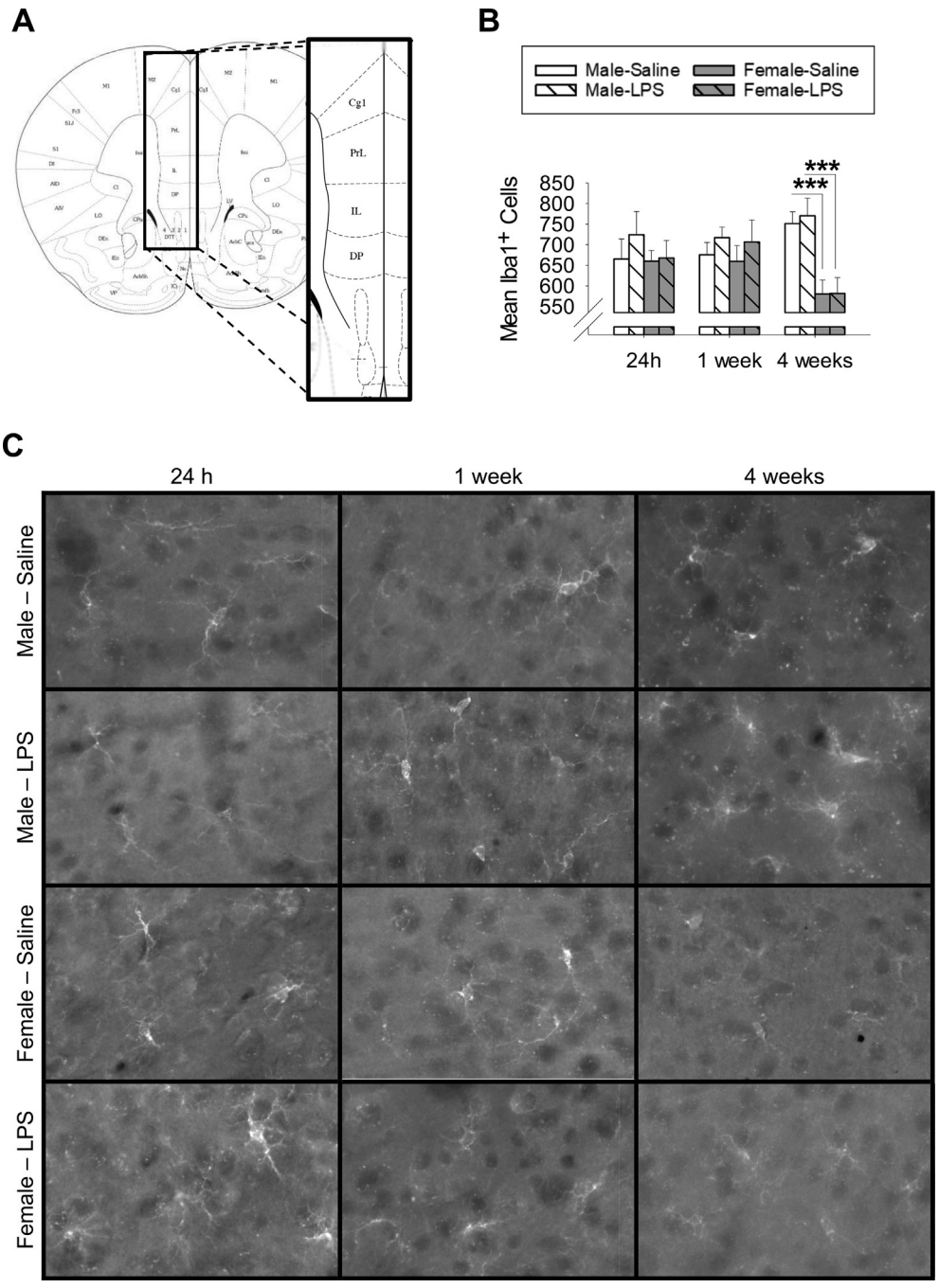

Fig. 6. Microglial expression in the mPFC. *Note.* Schematic drawing depicting the region of interest in the (i.e., bregma: +1.78 mm) (Franklin and Paxinos, 2007) (**A**). Data presented as mean (±*SEM*) total Iba1$^+$ cells counted in the mPFC (**B**). Photomicrographs of Iba1$^+$ cells in the mPFC from the experimental groups from the three time-points (i.e., 24 h, one week, and four weeks post-treatment) (**C**). Asterisks depict significant sex and treatment differences (* = $p <$ .05, ** = $p <$ .01, *** = $p <$ .001).

males compared to their saline-treated and female counterparts (*MD* = 0.38, *SE* = 0.14, p = .010 and *MD* = 0.38, *SE* = 0.14, p = .010, respectively). Non-neuronal apoptosis in the mPFC was similar across groups at each time-point (all $p >$ .05).

3.8. LPS-induced changes in microglial expression in the PVN

Microglial expression in the PVN revealed a significant time x sex × treatment interaction ($F_{(2,\ 84)} = 5.64$, p = .005, $\eta_p^2 = 0.118$) and significant main effects of treatment ($F_{(1,\ 84)} = 5.63$, p = .020, $\eta_p^2 = 0.063$) and sex ($F_{(1,\ 84)} = 10.42$, p = .002, $\eta_p^2 = 0.110$) (see Fig. 8B). During LPS-induced sickness, LPS-treated females had significantly more Iba1$^+$ cells in the PVN than their male counterparts (*MD* = 32.69, *SE* = 12.42, p = .010). Iba1$^+$ cell expression one week post-treatment was significantly lower among saline-treated males compared to LPS-treated males (*MD* = −32.38, *SE* = 12.42, p = .011) and saline-treated females (*MD* = −36.75, *SE* = 12.42, p = .004). Iba1$^+$ cell numbers in the adult PVN were significantly higher among LPS-treated females relative to saline-treated females and LPS-treated males (*MD* = 35.13, *SE* = 12.42, p = .006 and *MD* = 28.25, *SE* = 12.42, p = .025, respectively).

3.9. Time-related sex and treatment effects on microglial morphology in the PVN

Fractal analyses in the PVN (see Fig. 9A–E) revealed a significant sex × treatment interaction for D_B ($F_{(1,\ 84)} = 8.63$, p = .004, $\eta_p^2 = 0.093$) and density ($F_{(1,\ 84)} = 4.89$, p = .030, $\eta_p^2 = 0.055$) and a significant time × treatment interaction for lacunarity ($F_{(1,\ 84)} = 3.42$, p = .037, $\eta_p^2 = 0.075$). A main effect of treatment was also observed for lacunarity ($F_{(1,\ 84)} = 4.26$, p = .042, $\eta_p^2 = 0.048$). The ANOVAs failed to reveal statistically

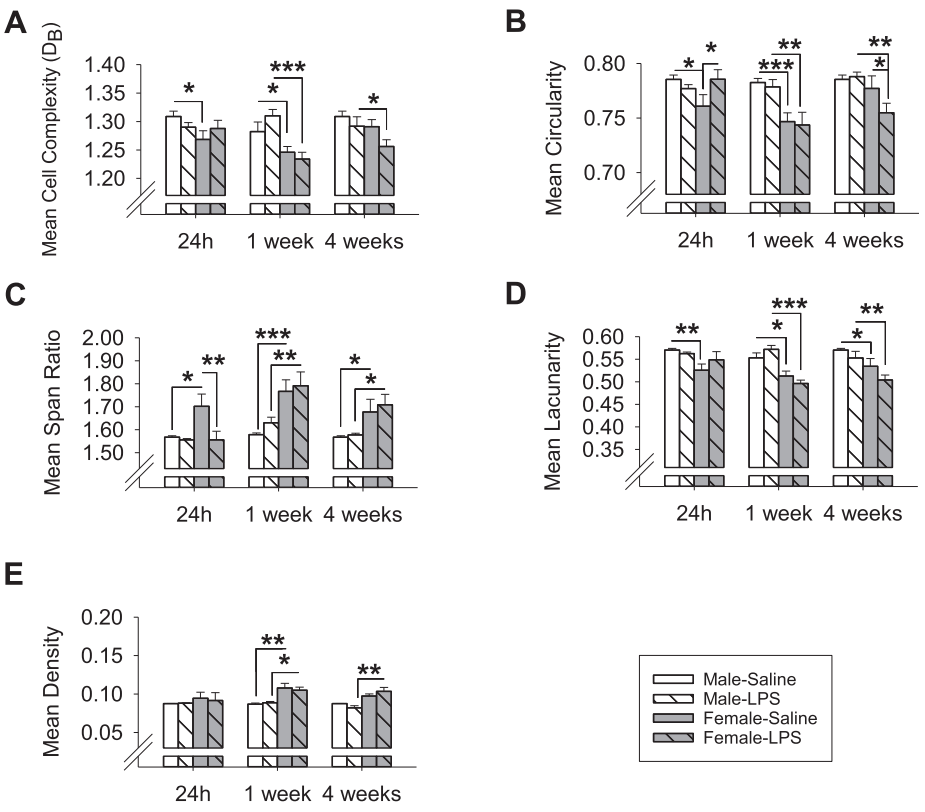

Fig. 7. Sex and treatment differences in microglial morphology in the mPFC.
Note. The figures depict group means (±*SEM*) in fractal analyses (i.e., fractal dimension [**A**], circularity [**B**], span ratio [**C**], lacunarity [**D**], and density [**E**]) of microglia in the mPFC 24 h, one week, and four weeks post-treatment. Asterisks denote significant sex and treatment differences (* = $p < .05$, ** = $p < .01$, *** = $p < .001$).

Table 3
Caspase-3-dependent apoptosis in the mPFC.

Cell	Time post-treatment	Males		Females	
		Saline-treated	LPS-treated	Saline-treated	LPS-treated
Caspase-3$^+$	24 h	.25 (1.60)	.00 (.00)	.00 (.00)	.00 (.00)
	1 week	.25 (1.60)	.00 (.00)	.00 (.00)	.00 (.00)
	4 weeks	.00 (.00)	.38 (.26)	.00 (.00)	.00 (.00)
Caspase-3$^+$/ NeuN$^+$	24 h	.25 (1.60)	.00 (.00)	.00 (.00)	.00 (.00)
	1 week	.25 (1.60)	.00 (.00)	.00 (.00)	.00 (.00)
	4 weeks	.00 (.00)	.38 (.26)	.00 (.00)	.00 (.00)
Caspase-3$^+$/ NeuN$^-$	24 h	.00 (.00)	.00 (.00)	.00 (.00)	.00 (.00)
	1 week	.00 (.00)	.00 (.00)	.00 (.00)	.00 (.00)
	4 weeks	.00 (.00)	.00 (.00)	.00 (.00)	.00 (.00)

Note. Data present group means (±*SEM*) of total caspase-3$^+$, caspase-3$^+$/NeuN$^+$ (i.e., neuronal), and caspase-3$^+$/NeuN$^-$ (i.e., non-neuronal) cells counted in the mPFC. Asterisks denote significant sex and treatment differences (* = $p < .05$, ** = $p < .01$, *** = $p < .001$).

significant main effects and interactions for circularity and span ratio of microglia in the PVN (all $p > .05$).

The morphometric features of microglia in the PVN were similar across groups 24 h post-treatment (all $p > .05$). Following symptomatic recovery from treatment, LPS-treated females had significantly higher D_B and lacunarity values relative to saline-treated females ($MD = 0.04$, $SE = 0.02$, $p = .023$ and $MD = 0.04$, $SE = 0.01$, $p = .004$, respectively). Saline-treated males also showed significantly higher D_B and density values than LPS-treated males ($MD = 0.04$, $SE = 0.02$, $p = .026$ and $MD = 0.03$, $SE = 0.01$, $p = .032$, respectively) and saline-treated females ($MD = 0.06$, $SE = 0.02$, $p = .001$ and $MD = 0.04$, $SE = 0.01$, $p = .006$, respectively) at this time-point. During adulthood, lacunarity values were significantly higher among saline-treated males relative to saline-treated females ($MD = 0.03$, $SE = 0.01$, $p = .033$).

3.10. Apoptosis of neuronal and non-neuronal cells in the PVN

Caspase-3$^+$ cells were not detected in the PVN of any groups at any of the time-points.

3.11. Sex and treatment differences in whole-brain and regional BBB disruption

3.11.1. Regional

^{14}C-sucrose brain/serum ratios in cerebellar, hippocampal, hypothalamic, and PFC tissue 24 h post-treatment failed to identify any significant interactions and main effects (all $p > .05$) (see Fig. 10A–D).

3.11.2. Whole-brain

^{14}C-sucrose whole-brain/serum ratios demonstrated a significant time x sex × treatment interaction ($F_{(1, 56)} = 4.55$, $p = .037$, $\eta^2_p = 0.075$) and a significant main effect of treatment ($F_{(1, 56)} = 5.75$, $p = .020$, $\eta^2_p = 0.093$) (see Fig. 10E and F). LPS-treated females had significantly higher ^{14}C-sucrose whole-brain/serum ratios 24 h post-treatment than their saline-treated and male counterparts ($MD = 10.09$, $SE = 3.61$, $p = .007$ and $MD = 11.01$, $SE = 3.61$, $p = .003$, respectively). ^{14}C-sucrose whole brain/serum ratios were similar across groups one week post-treatment (all $p > .05$).

4. Discussion

Pubertal CD-1 mice displayed sex-specific patterns of LPS-induced changes to BBB permeability, microglia expression and morphology (see Table 4), and caspase-3-dependent apoptosis in brain regions involved in stress and cognition. The acute effects of systemic LPS on the pubertal neuroimmune system were specific to females (i.e., altered microglial morphology in the hippocampus and the mPFC, increased hippocampal apoptosis, and global BBB disruption). Despite symptomatic recovery from LPS, microglia increased in number in the PVN of males and in the hippocampus of females and displayed several

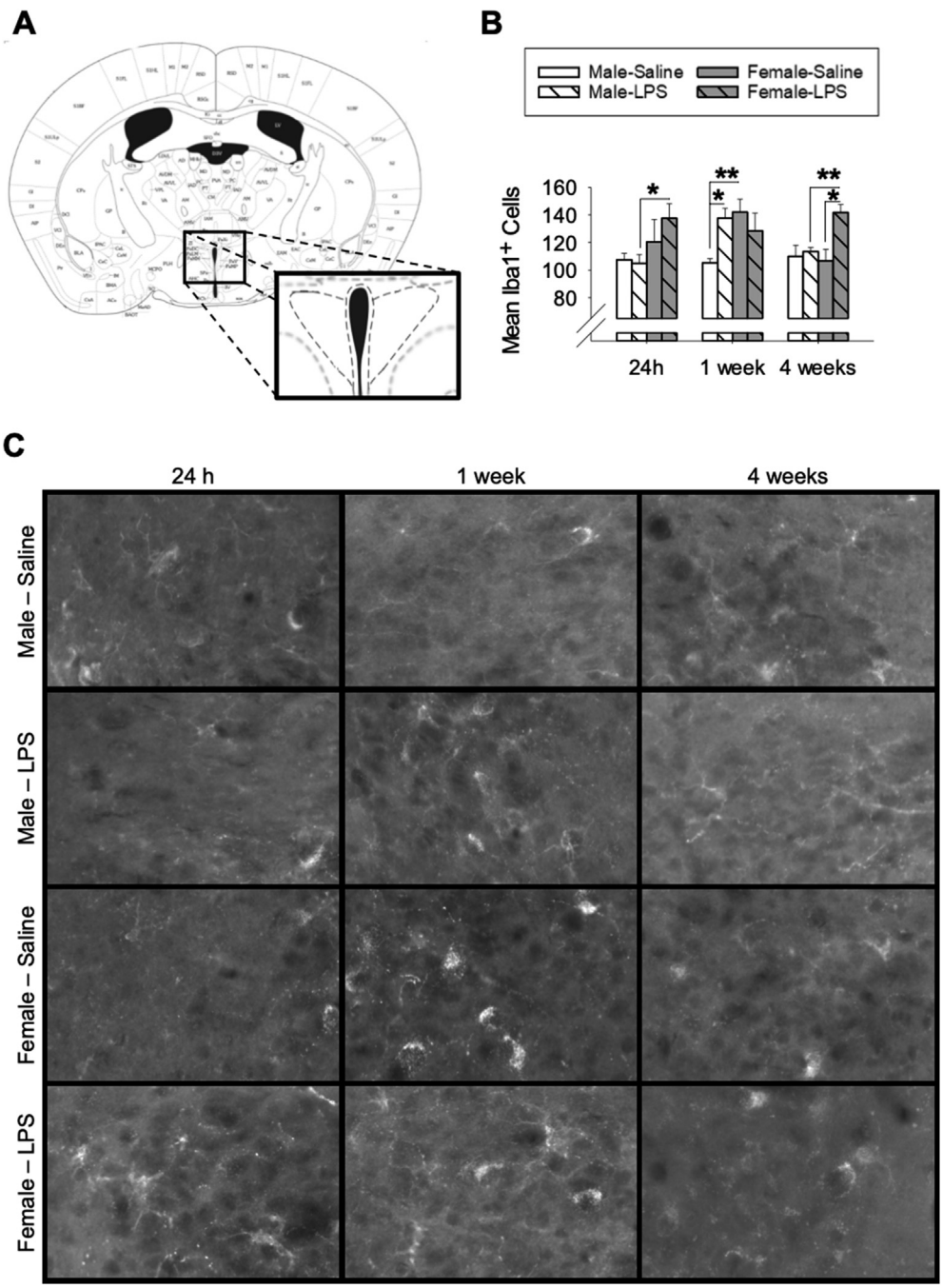

Fig. 8. Microglial expression in the PVN. *Note.* Schematic drawing depicting the region of interest in the (i.e., bregma: −0.82 mm) (Franklin and Paxinos, 2007) (**A**). Data presented as mean (±*SEM*) total Iba1$^+$ cells counted in the PVN (**B**). Photomicrographs of Iba1$^+$ cells in the PVN from the experimental groups from the three time-points (i.e., 24 h, one week, and four weeks post-treatment) (**C**). Asterisks depict significant sex and treatment differences (* = $p < .05$, ** = $p < .01$, *** = $p < .001$).

morphometric changes in the PVN of both sexes and in the hippocampus of females one week post-treatment. Four weeks post-treatment, LPS-treated males showed apoptosis of mPFC neurons and heightened expression of microglia in the CA3 region of the hippocampus, whereas their female counterparts showed increased microglial expression in the PVN and altered morphology of microglia in the mPFC and in the hippocampus. The pubertal neuroimmune system's response to systemic LPS, especially within microglia, highlight the sex-specific nature of this critical period for sexual maturation and the sex-specific vulnerability of these interconnected brain systems.

Unlike BBB permeability and caspase-3 activity, microglia displayed baseline region-specific sex differences spanning from puberty through adulthood. Young (i.e., six- and seven-week-old) females had lower microglial expression in the hippocampus than age-matched males, though this sex difference disappeared by adulthood (i.e., ten weeks of age). Microglial expression increased temporarily in the PVN of females at seven weeks of age and diverged significantly between the sexes in the mPFC during adulthood. Fractal analyses of young saline-treated mice identified larger hippocampal microglia, structurally simpler and elongated microglia in the mPFC, and smaller, less structurally complex microglia in the PVN among females relative to age-matched males. Hippocampal microglia remained larger in females during adulthood, and microglia in the hippocampus and the mPFC of adult mice were more elongated in females relative to males. Sex differences in PVN lacunarity among adult controls imply less bushiness/ramification of PVN microglia in males relative to females. These sex differences in microglia are likely secondary to the sex differences in age of pubertal onset and the ensuing developmental changes towards sexual maturity (Schulz et al., 2009; Sisk, 2016; Sisk and Foster, 2004). Similar sex and region differences in microglia during earlier critical periods (Lenz et al., 2013; Schwarz et al.,

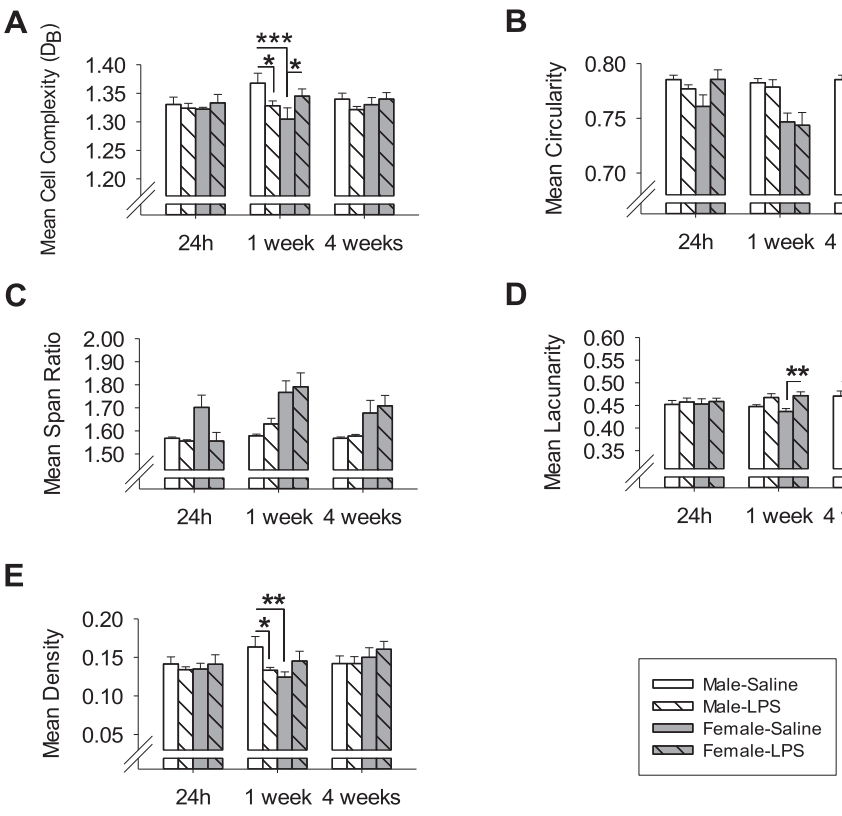

Fig. 9. Sex and treatment differences in microglial morphology in the PVN.
Note. The figures depict group means (±*SEM*) in fractal analyses (i.e., fractal dimension [**A**], circularity [**B**], span ratio [**C**], lacunarity [**D**], and density [**E**]) of microglia in the PVN 24 h, one week, and four weeks post-treatment. Asterisks denote significant sex and treatment differences (* = $p < .05$, ** = $p < .01$, *** = $p < .001$).

2012) are thought to arise in part from sex differences in the organizational and activational effects of fluctuating gonadal steroid hormone levels (Crain et al., 2013; Sierra et al., 2008). The reactivation of the hypothalamic-pituitary-gonadal axis at pubertal onset leads to similar changes in circulating levels of androgenic and estrogenic steroids secreted by the testes and the ovaries (Herbison, 2016; Sisk and Foster, 2004). Therefore, it is plausible that sex differences in the influx of androgens, estrogens, and progesterone at pubertal onset influences microglial expression and phenotype during this critical period (Herbison, 2016; Sisk and Foster, 2004).

Systemic LPS was able to alter baseline number and morphology of pubertal microglia in a sex-specific manner. During LPS-induced sickness, females showed an increase in hippocampal cell complexity and increased circularity and elongation of microglia in the mPFC. Pubertal LPS treatment eliminated baseline sex differences in expression and certain morphological features of hippocampal and PVN microglia seen in seven-week-old mice. The LPS-induced changes to microglial morphology in the PVN one week post-treatment point towards a female-specific transition to a more "activated" microglial state despite symptomatic recovery from LPS-induced sickness. Pubertal LPS treatment also removed the sex difference in CA3 microglial expression during adulthood and increased PVN microglial expression in adult females. Relative to their saline-treated counterparts, adult females treated with LPS during puberty also showed less circularity in mPFC microglia and greater cell complexity and lacunarity in hippocampal microglia.

Aside from baseline sex differences in microglia during this critical period, pubertal females may have been more vulnerable than their male counterparts to LPS-induced changes to microglia because of sex differences in BBB integrity. Systemic LPS disrupts BBB permeability by interfering with the paracellular and transcellular pathways of transport (Banks et al., 2015; Erickson et al., 2018; Nishioku et al., 2009). We found that systemic LPS significantly increased global BBB permeability during sickness in pubertal females but not males. Given that BBB permeability in the hippocampus, cerebellum, hypothalamus, and PFC were grossly intact during LPS-induced sickness in both sexes, this global BBB disruption likely resulted from additive effects of non-significant changes to BBB permeability across brain regions. This increased global BBB permeability is a double-edged sword because infiltrating circulating immune factors (e.g., peripheral leukocytes, pro- and anti-inflammatory cytokines) may assist with wound healing and debris clearance in the CNS but can also lead to maladaptive immune activation, immune-mediated cellular damage and dysfunction, and increases in intracranial pressure (Varatharaj and Galea, 2017). Follow-up research is needed to confirm the functional consequences of this sex-specific effect of pubertal immune challenge on BBB permeability.

Pubertal fluctuations in gonadal steroid hormones likely contributed to the sex-specific responses of the pubertal neuroimmune network to systemic LPS. Circulating androgenic and estrogenic steroids moderate the neuroimmune network's responses via direct and indirect means (Dantzer, 2017; Hampl et al., 2015; Robison et al., 2019). In general, estrogens tend to dilate cerebrovascular tone, increase cerebral flow, and facilitate immune-supporessing or anti-inflammatory responses in the brain and cerebrovasculature (Brown et al., 2007; Gonzales et al., 2005, 2008; Gottfried-Blackmore et al., 2008; Kipp et al., 2012; Krause et al., 2002; Ospina et al., 2003, 2004; Sunday et al., 2006). Androgens tend to constrict vascular tone and enhance immune responses (i.e., pro-inflammatory effects). Consistent with our findings, the organizational and activational effects of circulating hormones also extend to the activation of molecular cell death pathways during inflammatory events, fostering a female bias in caspase-dependent apoptosis at younger ages (Arai et al., 1996; Liu et al., 2009; Nuñez et al., 2001; Penaloza et al., 2009; Rau et al., 2003). However, recent evidence of estradiol-mediated amplification of microglial, cytokine, and thermoregulatory responses to systemic LPS in pubertal female C57Bl/6 mice suggests age-related hormonal influences on the neuroimmune system's functioning (Velez-Perez, 2020). Therefore, further investigation is warranted to elucidate the role of circulating gonadal steroid hormones in the sex-specific vulnerability and reactivity of the pubertal neuroimmune network.

The functional significance of the LPS-induced changes to microglial structure reported here are unclear. Morphometric analyses revealed sex-

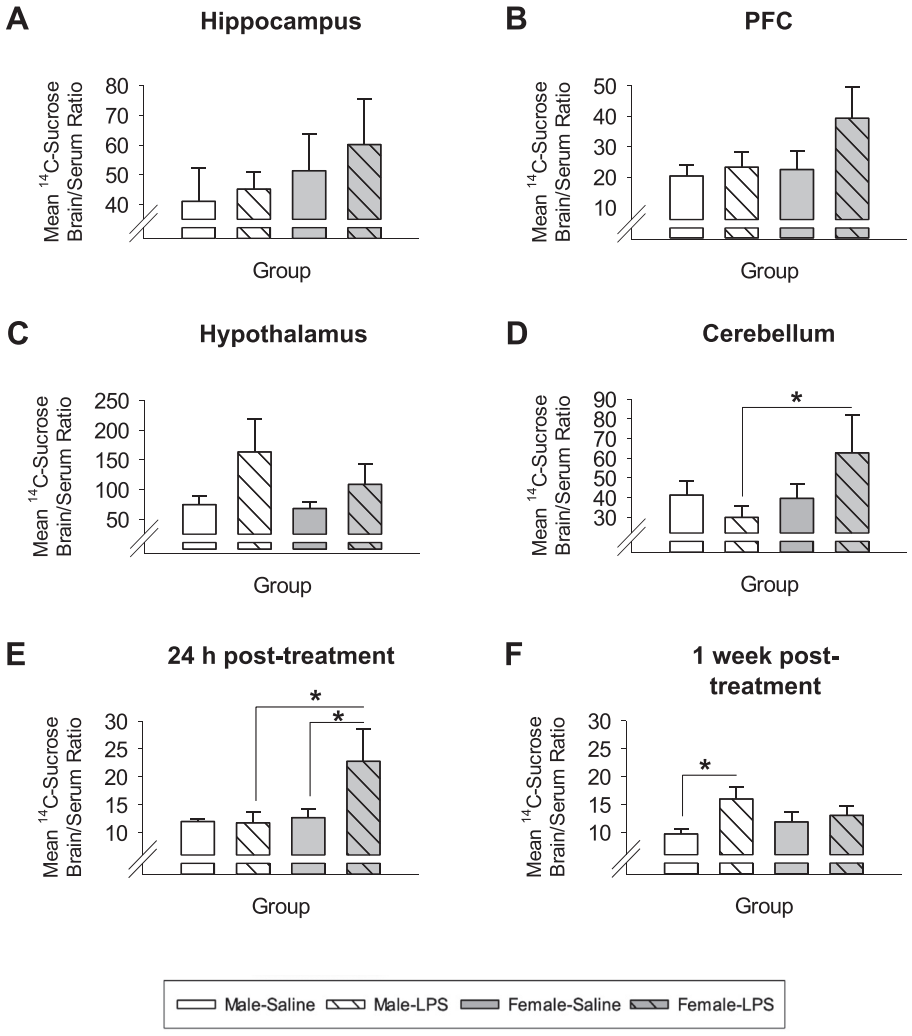

Fig. 10. Sex and treatment differences in global and regional BBB permeability.
Note. Data presented as mean (±*SEM*) ^{14}C-sucrose whole brain/serum (μL/g) ratios in the hippocampus (**A**), PFC (**B**), hypothalamus (**C**), cerebellum (**D**) 24 h post-treatment and in the whole-brain 24 h (**E**) and one week (**F**) post-treatment. Asterisks denote significant pairwise comparisons (* = $p < .05$, ** = $p < .01$, *** = $p < .001$).

and region-dependent changes to microglial morphology following pubertal LPS treatment. Among LPS-treated mice, females were more prone to morphometric changes, several of which are consistent with an increase in "activational" state. For example, the increased circularity and elongation of microglial cells in the mPFC of females during LPS-induced sickness point towards a shift in morphology towards the more activated "rod-like" form (Morrison et al., 2017; Taylor et al., 2014). Although fractal analyses captured the subtle LPS-induced changes to microglial structure that categorical, qualitative approaches cannot (e.g., Fernández-Arjona et al., 2017; Morrison et al., 2017; Soltys et al., 2001), this approach does not allude to the phenotypic polarization of microglia. The duality in microglia-mediated neuroinflammatory responses (i.e., simultaneous secretion of pro-inflammatory and pro-repair mechanisms of inflammation) complicate the functional translation of these morphological changes on the local microenvironment (Giordano et al., 2021; Loane and Kumar, 2016). Given that the magnitude of this duality also differs between the sexes (Crain et al., 2013; Guneykaya et al., 2018; Hanamsagar et al., 2017; Lively et al., 2018; Villa et al., 2018), additional investigations into the kinds of inflammatory responses employed by pubertal microglia are needed to provide functional context to our findings.

Immune-mediated perturbations during stress-sensitive critical periods like puberty have widespread implications for health. Sex differences in stress responses (Oyola and Handa, 2017) during this critical postnatal period may explain sex biases in the pathogenesis of stress-related disorders that appear during puberty or early adulthood but do not originate in the pre-/post-natal periods or during adulthood (Angold and Costello, 2006; Marcotte et al., 2002). Preclinical and clinical models generally show a strong positive relationship between stress burden during puberty and risk for internalizing and externalizing disorders, reactivity to future stressors, and cognitive functioning in young adulthood (e.g., Angold et al., 1998; Byrne et al., 2017; Ellis et al., 2019; Graber, 2013; Hamilton et al., 2014). Our findings add to this literature by highlighting sex differences in the vulnerability of the pubertal neuroimmune response, particularly within microglia, across brain regions involved in stress responses and cognitive functioning. Microglia play critical roles in immune responses, homeostatic process (e.g., debris clearance), the shaping of immature neural networks, and programming of adult behaviours (Lenz and Nelson, 2018; Li and Barres, 2018; Mottahedin et al., 2017; Nelson et al., 2019; Wolf et al., 2016). Therefore, the residual effects of LPS-induced sickness on microglial expression and morphology in the hippocampus, mPFC, and the PVN suggest mechanistic involvement of these cells in the sex-specific outcomes of pubertal LPS on related behaviours (i.e., stress and immune responses [Cai et al., 2016; Girard-Joyal et al., 2015; Sharma et al., 2019]; depression-like behaviours [Murray et al., 2019]; spatial retention errors on hippocampus-dependent tasks [Kolmogorova et al., 2019]; reactivity to novel stressors and expression of anxiety-like behaviours (Murray et al., 2019]).

Table 4
Summary of key findings in microglia cells.

Region	Summary of key findings
Hippocampus	*Counts:* • The baseline male-skewed expression of hippocampal microglia during puberty disappears by early adulthood. Developmental sex differences in microglia numbers were also observed in hippocampal subregions. • Pubertal LPS temporarily increased total microglial numbers in females (i.e., one week post-treatment) and altered microglial numbers in a region- and sex-specific manner. Males were protected from acute LPS-induced changes to microglial expression. *Morphology:* • Among controls, young males showed larger hippocampal microglia relative to their female counterparts. Microglia were more structurally complex and larger in adult females relative to adult males. • Pubertal LPS increased cell complexity in females during sickness and eliminated several baseline morphological sex differences one week post-treatment. During adulthood, LPS-treated females showed greater cell complexity and lacunarity in hippocampal microglia than their saline-treated counterparts. Males were protected from acute and enduring LPS-induced changes to morphology.
mPFC	*Counts:* • Baseline microglial expression diverged during adulthood (i.e., total microglial expression increased in males and decreased in females relative to their younger counterparts). • Pubertal LPS did not impact baseline microglial expression in males and females. *Morphology:* • Several baseline sex differences in mPFC microglia were observed from puberty through adulthood. • Females showed elongation of mPFC microglia during LPS-induced sickness. Pubertal LPS decreased baseline circularity of microglia in adult females.
PVN	*Counts:* • Baseline microglial expression increased temporarily in the PVN of females at seven weeks of age. • Pubertal LPS temporarily increased microglial expression in males at seven weeks of age. LPS-treated females showed an increased in PVN microglial expression in adulthood. *Morphology:* • Young female controls showed smaller, less structurally complex microglia in the PVN relative to their male counterparts. Adult males showed greater lacunarity (i.e., reduced bushiness/ramification) in PVN microglia than adult females. • Pubertal LPS temporarily altered morphology in males and females. These LPS-induced changes one week post-treatment suggest a female-specific transition to a more "activated" microglial state despite symptomatic recovery from LPS-induced sickness.

4.1. Conclusions

This study examined whether the neuroimmune network contributes to the sex-specific outcomes of a systemic immune challenge during the stress-sensitive pubertal period. The female-specific BBB disruption appears to moderate some of the sex-specific effects of pubertal LPS on microglial expression and morphology in brain regions for stress regulation and cognitive functioning. The residual effects of LPS-induced sickness highlight the stress sensitivity of pubertal microglia and the sex- and region-specific nature of this vulnerability. These significant sex differences in the pubertal neuroimmune system may explain some sex biases in stress-related disorders of brain and behaviour that arise during adulthood.

Funding sources

This work was supported by the Natural Sciences and Engineering Research Council of Canada [grant number RGPIN-05570-2014] and the Ontario Graduate Scholarship.

Declaration of competing interest

We have no conflict of interest to declare.

Acknowledgements

The authors would like to extend their deepest gratitude to the staff of the Animal Care and Veterinary Service of the University of Ottawa for their excellent technical support. We are also grateful to Dr. Jean-Michel Weber and his student Ms. Mais Jubouri at the University of Ottawa for their generosity with their scintillation counter. We thank Dr. William A. Banks for sharing his protocol with us and for answering questions related to blood-brain barrier disruption assessment. We would also like to thank the volunteers and students of the NISE lab who helped see this project through.

References

Abbott, N.J., Rönnbäck, L., Hansson, E., 2006. Astrocyte–endothelial interactions at the blood–brain barrier. Nat. Rev. Neurosci. 7, 41–53. https://doi.org/10.1038/nrn1824.
Abdi, H., 2007. Bonferroni and Sidak corrections for multiple comparisons. Encyclopedia of Measurement and Statistics 103–107.
Abi-Ghanem, C., Robison, L.S., Zuloaga, K.L., 2020. Androgens' effects on cerebrovascular function in health and disease. Biol. Sex Differ. 11, 35. https://doi.org/10.1186/s13293-020-00309-4.
Alfonso-Loeches, S., Pascual, M., Guerri, C., 2013. Gender differences in alcohol-induced neurotoxicity and brain damage. Toxicology 311, 27–34. https://doi.org/10.1016/j.tox.2013.03.001.
Angold, A., Costello, E.J., 2006. Puberty and depression. Child and Adolescent Psychiatric Clinics of North America 15, 919–937. https://doi.org/10.1016/j.chc.2006.05.013.
Angold, A., Costello, E.J., Worthman, C.M., 1998. Puberty and depression: the roles of age, pubertal status and pubertal timing. Psychol. Med. 28, 51–61. https://doi.org/10.1017/S003329179700593X.
Arai, Y., Sekine, Y., Murakami, S., 1996. Estrogen and apoptosis in the developing sexually dimorphic preoptic area in female rats. Neurosci. Res. 25, 403–407. https://doi.org/10.1016/0168-0102(96)01070-x.
Banks, W.A., Gray, A.M., Erickson, M.A., Salameh, T.S., Damodarasamy, M., Sheibani, N., Meabon, J.S., Wing, E.E., Morofuji, Y., Cook, D.G., Reed, M.J., 2015. Lipopolysaccharide-induced blood-brain barrier disruption: roles of cyclooxygenase, oxidative stress, neuroinflammation, and elements of the neurovascular unit. J. Neuroinflammation 12, 223. https://doi.org/10.1186/s12974-015-0434-1.
Brown, C.M., Xu, Q., Okhubo, N., Vitek, M.P., Colton, C.A., 2007. Androgen-mediated immune function is altered by the apolipoprotein E gene. Endocrinology 148, 3383–3390. https://doi.org/10.1210/en.2006-1200.
Byrne, M.L., Whittle, S., Vijayakumar, N., Dennison, M., Simmons, J.G., Allen, N.B., 2017. A systematic review of adrenarche as a sensitive period in neurobiological development and mental health. Dev Cogn Neurosci 25, 12–28. https://doi.org/10.1016/j.dcn.2016.12.004.
Cai, K.C., van Mil, S., Murray, E., Mallet, J.-F., Matar, C., Ismail, N., 2016. Age and sex differences in immune response following LPS treatment in mice. Brain Behav. Immun. 58, 327–337. https://doi.org/10.1016/j.bbi.2016.08.002.
Crain, J.M., Nikodemova, M., Watters, J.J., 2013. Microglia express distinct M1 and M2 phenotypic markers in the postnatal and adult central nervous system in male and female mice. J. Neurosci. Res. 91, 1143–1151. https://doi.org/10.1002/jnr.23242.
Cunningham, C., Wilcockson, D.C., Campion, S., Lunnon, K., Perry, V.H., 2005. Central and systemic endotoxin challenges exacerbate the local inflammatory response and increase neuronal death during chronic neurodegeneration. J. Neurosci. 25, 9275–9284. https://doi.org/10.1523/jneurosci.2614-05.2005.
Dantzer, R., 2017. Neuroimmune interactions: from the brain to the immune system and vice versa. Physiol. Rev. 98, 477–504. https://doi.org/10.1152/physrev.00039.2016.
Du, L., Bayir, H., Lai, Y., Zhang, X., Kochanek, P.M., Watkins, S.C., Graham, S.H., Clark, R.S.B., 2004. Innate gender-based proclivity in response to cytotoxicity and programmed cell death pathway. J. Biol. Chem. 279, 38563–38570. https://doi.org/10.1074/jbc.m405461200.
Duckles, S.P., Krause, D.N., 2007. Cerebrovascular effects of oestrogen: multiplicity of action. Clin. Exp. Pharmacol. Physiol. 34, 801–808. https://doi.org/10.1111/j.1440-1681.2007.04683.x.
Ellis, R., Fernandes, A., Simmons, J.G., Mundy, L., Patton, G., Allen, N.B., Whittle, S., 2019. Relationships between adrenarcheal hormones, hippocampal volumes and depressive symptoms in children. Psychoneuroendocrinology 104, 55–63. https://doi.org/10.1016/j.psyneuen.2019.02.016.

Elmore, S., 2007. Apoptosis: a review of programmed cell death. Toxicol. Pathol. 35, 495–516. https://doi.org/10.1080/01926230701320337.
Engelhardt, B., Liebner, S., 2014. Novel insights into the development and maintenance of the blood–brain barrier. Cell Tissue Res. 355, 687–699. https://doi.org/10.1007/s00441-014-1811-2.
Erdö, F., Denes, L., Lange, E. de, 2016. Age-associated physiological and pathological changes at the blood–brain barrier: a review. J. Cerebr. Blood Flow Metabol. 37, 4–24. https://doi.org/10.1177/0271678x16679420.
Erickson, M.A., Banks, W.A., 2019. Age-associated changes in the immune system and blood–brain barrier functions. Int. J. Mol. Sci. 20, 1632. https://doi.org/10.3390/ijms20071632.
Erickson, M.A., Liang, W.S., Fernandez, E.G., Bullock, K.M., Thysell, J.A., Banks, W.A., 2018. Genetics and sex influence peripheral and central innate immune responses and blood-brain barrier integrity. PloS One 13, e0205769. https://doi.org/10.1371/journal.pone.0205769.
Fernández-Arjona, M. del M., Grondona, J.M., Granados-Durán, P., Fernández-Llebrez, P., López-Ávalos, M.D., 2017. Microglia morphological categorization in a rat model of neuroinflammation by hierarchical cluster and principal components analysis. Front. Cell. Neurosci. 11, 235. https://doi.org/10.3389/fncel.2017.00235.
Franklin, K., Paxinos, G., 2007. The Mouse Brain in Stereotaxic Coordinates, third ed.
Giordano, K.R., Denman, C.R., Dubisch, P.S., Akhter, M., Lifshitz, J., 2021. An update on the rod microglia variant in experimental and clinical brain injury and disease. Brain Commun 3. https://doi.org/10.1093/braincomms/fcaa227 fcaa227–fcaa227.
Girard-Joyal, O., Faragher, A., Bradley, K., Kane, L., Hrycyk, L., Ismail, N., 2015. Age and sex differences in c-Fos expression and serum corticosterone concentration following LPS treatment. Neuroscience 305, 293–301. https://doi.org/10.1016/j.neuroscience.2015.06.035.
Girard-Joyal, O., Ismail, N., 2017. Effect of LPS treatment on tyrosine hydroxylase expression and Parkinson-like behaviors. Horm. Behav. 89, 1–12. https://doi.org/10.1016/j.yhbeh.2016.12.009.
Gonzales, R., Razmara, A., Sunday, L., Krause, D., Duckles, S., 2005. Gonadal hormones modulate LPS-induced inflammatory markers in rat cerebral blood vessels. J. Cerebr. Blood Flow Metabol. 25 https://doi.org/10.1038/sj.jcbfm.9591524.0111. S111–S111.
Gonzales, R.J., Duckles, S.P., Krause, D.N., 2008. Dihydrotestosterone stimulates cerebrovascular inflammation through NFκB, modulating contractile function. J. Cerebr. Blood Flow Metabol. 29, 244–253. https://doi.org/10.1038/jcbfm.2008.115.
Gottfried-Blackmore, A., Sierra, A., Jellinck, P.H., McEwen, B.S., Bulloch, K., 2008. Brain microglia express steroid-converting enzymes in the mouse. J. Steroid Biochem. Mol. Biol. 109, 96–107. https://doi.org/10.1016/j.jsbmb.2007.12.013.
Graber, J.A., 2013. Pubertal timing and the development of psychopathology in adolescence and beyond. Horm. Behav. 64, 262–269. https://doi.org/10.1016/j.yhbeh.2013.04.003.
Guneykaya, D., Ivanov, A., Hernandez, D.P., Haage, V., Wojtas, B., Meyer, N., Maricos, M., Jordan, P., Buonfiglioli, A., Gielniewski, B., Ochocka, N., Cömert, C., Friedrich, C., Artiles, L.S., Kaminska, B., Mertins, P., Beule, D., Kettenmann, H., Wolf, S.A., 2018. Transcriptional and translational differences of microglia from male and female brains. Cell Rep. 24, 2773–2783. https://doi.org/10.1016/j.celrep.2018.08.001 e6.
Hamilton, J.L., Hamlat, E.J., Stange, J.P., Abramson, L.Y., Alloy, L.B., 2014. Pubertal timing and vulnerabilities to depression in early adolescence: differential pathways to depressive symptoms by sex. J. Adolesc. 37, 165–174. https://doi.org/10.1016/j.adolescence.2013.11.010.
Hampl, R., Bičíková, M., Sosvorová, L., 2015. Hormones and the blood-brain barrier. Horm. Mol. Biol. Clin. Invest. 21, 159–164. https://doi.org/10.1515/hmbci-2014-0042.
Hanamsagar, R., Alter, M.D., Block, C.S., Sullivan, H., Bolton, J.L., Bilbo, S.D., 2017. Generation of a microglial developmental index in mice and in humans reveals a sex difference in maturation and immune reactivity. Glia 65, 1504–1520. https://doi.org/10.1002/glia.23176.
Herbison, A.E., 2016. Control of puberty onset and fertility by gonadotropin-releasing hormone neurons. Nat. Rev. Endocrinol. 12, 452–466. https://doi.org/10.1038/nrendo.2016.70.
Holder, M.K., Blaustein, J.D., 2014. Puberty and adolescence as a time of vulnerability to stressors that alter neurobehavioral processes. Front. Neuroendocrinol. 35, 89–110. https://doi.org/10.1016/j.yfrne.2013.10.004.
Hoogland, I.C.M., Houbolt, C., Westerloo, D.J. van, Gool, W.A. van, Beek, D. van de, 2015. Systemic inflammation and microglial activation: systematic review of animal experiments. J. Neuroinflammation 12, 114. https://doi.org/10.1186/s12974-015-0332-6.
Ismail, N., Kumlin, A.M., Blaustein, J.D., 2013. A pubertal immune challenge alters the antidepressant-like effects of chronic estradiol treatment in inbred and outbred adult female mice. Neuroscience 249, 43–52. https://doi.org/10.1016/j.neuroscience.2012.09.047.
Kane, L., Ismail, N., 2017. Puberty as a vulnerable period to the effects of immune challenges: focus on sex differences. Behav. Brain Res. 320, 374–382. https://doi.org/10.1016/j.bbr.2016.11.006.
Karperien, A., Ahammer, H., Jelinek, H.F., 2013. Quantitating the subtleties of microglial morphology with fractal analysis. Front. Cell. Neurosci. 7, 3. https://doi.org/10.3389/fncel.2013.00003.
Khan, M.S., Ali, T., Abid, M.N., Jo, M.H., Khan, A., Kim, M.W., Yoon, G.H., Cheon, E.W., Rehman, S.U., Kim, M.O., 2017. Lithium ameliorates lipopolysaccharide-induced neurotoxicity in the cortex and hippocampus of the adult rat brain. Neurochem. Int. 108, 343–354. https://doi.org/10.1016/j.neuint.2017.05.008.
Khan, M.S., Ali, T., Kim, M.W., Jo, M.H., Jo, M.G., Badshah, H., Kim, M.O., 2016. Anthocyanins protect against LPS-induced oxidative stress-mediated neuroinflammation and neurodegeneration in the adult mouse cortex. Neurochem. Int. 100, 1–10. https://doi.org/10.1016/j.neuint.2016.08.005.
Kipp, M., Berger, K., Clarner, T., Dang, J., Beyer, C., 2012. Sex steroids control neuroinflammatory processes in the brain: relevance for acute ischaemia and degenerative demyelination. J. Neuroendocrinol. 24, 62–70. https://doi.org/10.1111/j.1365-2826.2011.02163.x.
Kolmogorova, D., Murray, E., Ismail, N., 2017. Monitoring pathogen-induced sickness in mice and rats. Curr Protoc Mouse Biology 7, 65–76. https://doi.org/10.1002/cpmo.27.
Kolmogorova, D., Paré, C., Kostuck, S., Hudson, E.C., Lebel, N., Houlding, E., Gregory, J.G., Ismail, N., 2019. Pubertal immune stress transiently alters spatial memory processes in adulthood. Psychoneuro 102, 261–272. https://doi.org/10.1016/j.psyneuen.2018.12.224.
Krause, D.N., Duckles, S.P., Pelligrino, D.A., 2006. Influence of sex steroid hormones on cerebrovascular function. J. Appl. Physiol. 101, 1252–1261. https://doi.org/10.1152/japplphysiol.01095.2005.
Krause, D.N., Geary, G.G., McNeill, A.M., Ospina, J., Duckles, S.P., 2002. Impact of hormones on the regulation of cerebral vascular tone. Int Congr Ser 1235, 395–399. https://doi.org/10.1016/s0531-5131(02)00211-x.
Langen, U.H., Ayloo, S., Gu, C., 2019. Development and cell biology of the blood-brain barrier. Annu. Rev. Cell Dev. Biol. 35, 1–23. https://doi.org/10.1146/annurev-cellbio-100617-062608.
Laroche, J., Gasbarro, L., Herman, J.P., Blaustein, J.D., 2009a. Enduring influences of peripubertal/adolescent stressors on behavioral response to estradiol and progesterone in adult female mice. Endocrinology 150, 3717–3725. https://doi.org/10.1210/en.2009-0099.
Laroche, J., Gasbarro, L., Herman, J.P., Blaustein, J.D., 2009b. Reduced behavioral response to gonadal hormones in mice shipped during the peripubertal/adolescent period. Endocrinology 150, 2351–2358. https://doi.org/10.1210/en.2008-1595.
Lenz, K.M., Nelson, L.H., 2018. Microglia and beyond: innate immune cells as regulators of brain development and behavioral function. Front. Immunol. 9, 698. https://doi.org/10.3389/fimmu.2018.00698.
Lenz, K.M., Nugent, B.M., Haliyur, R., McCarthy, M.M., 2013. Microglia are essential to masculinization of brain and behavior. J. Neurosci. 33, 2761. https://doi.org/10.1523/JNEUROSCI.1268-12.2013.
Li, Q., Barres, B.A., 2018. Microglia and macrophages in brain homeostasis and disease. Nat. Rev. Immunol. 18, 225–242. https://doi.org/10.1038/nri.2017.125.
Ling, Z., Zhu, Y., Tong, C. wai, Snyder, J.A., Lipton, J.W., Carvey, P.M., 2006. Progressive dopamine neuron loss following supra-nigral lipopolysaccharide (LPS) infusion into rats exposed to LPS prenatally. Exp. Neurol. 199, 499–512. https://doi.org/10.1016/j.expneurol.2006.01.010.
Liu, F., Li, Z., Li, J., Siegel, C., Yuan, R., McCullough, L.D., 2009. Sex differences in caspase activation after stroke. Stroke 40, 1842–1848. https://doi.org/10.1161/strokeaha.108.538686.
Lively, S., Wong, R., Lam, D., Schlichter, L.C., 2018. Sex- and development-dependent responses of rat microglia to pro- and anti-inflammatory stimulation. Front. Cell. Neurosci. 12 https://doi.org/10.3389/fncel.2018.00433, 433–433.
Loane, D.J., Kumar, A., 2016. Microglia in the TBI brain: the good, the bad, and the dysregulated. Exp. Neurol. 275 (Pt 3), 316–327. https://doi.org/10.1016/j.expneurol.2015.08.018.
Marcotte, D., Fortin, L., Potvin, P., Papillon, M., 2002. Gender differences in depressive symptoms during adolescence: role of gender-typed characteristics, self-esteem, body image, stressful life events, and pubertal status. J. Emot. Behav. Disord. 10, 29–42. https://doi.org/10.1177/106342660201000104.
Morrison, H., Young, K., Qureshi, M., Rowe, R.K., Lifshitz, J., 2017. Quantitative microglia analyses reveal diverse morphologic responses in the rat cortex after diffuse brain injury. Sci Rep-uk 7, 13211. https://doi.org/10.1038/s41598-017-13581-z.
Mottahedin, A., Ardalan, M., Chumak, T., Riebe, I., Ek, J., Mallard, C., 2017. Effect of neuroinflammation on synaptic organization and function in the developing brain: implications for neurodevelopmental and neurodegenerative disorders. Front. Cell. Neurosci. 11, 190. https://doi.org/10.3389/fncel.2017.00190.
Murray, E., Sharma, R., Smith, K., Mar, K., Barve, R., Lukasik, M., Pirwani, A., Malette-Guyon, E., Lamba, S., Thomas, B., Sadeghi-Emamchaie, H., Liang, J., Mallet, J.-F., Matar, C., Ismail, N., 2019. Probiotic consumption during puberty mitigates LPS-induced immune responses and protects against stress-induced depression- and anxiety-like behaviors in adulthood in a sex-specific manner. Brain Behav. Immun. 81, 198–212. https://doi.org/10.1016/j.bbi.2019.06.016.
Nelson, L.H., Saulsbery, A.I., Lenz, K.M., 2019. Small cells with big implications: microglia and sex differences in brain development, plasticity and behavioral health. Prog. Neurobiol. 176, 103–119. https://doi.org/10.1016/j.pneurobio.2018.09.002.
Nishioku, T., Dohgu, S., Takata, F., Eto, T., Ishikawa, N., Kodama, K.B., Nakagawa, S., Yamauchi, A., Kataoka, Y., 2009. Detachment of brain pericytes from the basal lamina is involved in disruption of the blood–brain barrier caused by lipopolysaccharide-induced sepsis in mice. Cell. Mol. Neurobiol. 29, 309–316. https://doi.org/10.1007/s10571-008-9322-x.
Noh, H., Jeon, J., Seo, H., 2014. Systemic injection of LPS induces region-specific neuroinflammation and mitochondrial dysfunction in normal mouse brain. Neurochem. Int. 69, 35–40. https://doi.org/10.1016/j.neuint.2014.02.008.
Nuñez, J.L., Lauschke, D.M., Juraska, J.M., 2001. Cell death in the development of the posterior cortex in male and female rats. J. Comp. Neurol. 436, 32–41. https://doi.org/10.1002/cne.1051.
Olesen, K.M., Ismail, N., Merchasin, E.D., Blaustein, J.D., 2011. Long-term alteration of anxiolytic effects of ovarian hormones in female mice by a peripubertal immune challenge. Horm. Behav. 60, 318–326. https://doi.org/10.1016/j.yhbeh.2011.06.005.

Ospina, J.A., Brevig, H.N., Krause, D.N., Duckles, S.P., 2004. Estrogen suppresses IL-1β-mediated induction of COX-2 pathway in rat cerebral blood vessels. Am J Physiol-heart C 286, H2010–H2019. https://doi.org/10.1152/ajpheart.00481.2003.

Ospina, J.A., Duckles, S.P., Krause, D.N., 2003. 17β-Estradiol decreases vascular tone in cerebral arteries by shifting COX-dependent vasoconstriction to vasodilation. Am J Physiol-heart C 285, H241–H250. https://doi.org/10.1152/ajpheart.00018.2003.

Oyola, M.G., Handa, R.J., 2017. Hypothalamic-pituitary-adrenal and hypothalamic-pituitary-gonadal axes: sex differences in regulation of stress responsivity. Stress 20, 476–494. https://doi.org/10.1080/10253890.2017.1369523.

Penaloza, C., Estevez, B., Orlanski, S., Sikorska, M., Walker, R., Smith, C., Smith, B., Lockshin, R.A., Zakeri, Z., 2009. Sex of the cell dictates its response: differential gene expression and sensitivity to cell death inducing stress in male and female cells. Faseb. J. 23, 1869–1879. https://doi.org/10.1096/fj.08-119388.

Püntener, U., Booth, S.G., Perry, V.H., Teeling, J.L., 2012. Long-term impact of systemic bacterial infection on the cerebral vasculature and microglia. J. Neuroinflammation 9. https://doi.org/10.1186/1742-2094-9-146, 146–146.

Qin, L., Wu, X., Block, M.L., Liu, Y., Breese, G.R., Hong, J., Knapp, D.J., Crews, F.T., 2007. Systemic LPS causes chronic neuroinflammation and progressive neurodegeneration. Glia 55, 453–462. https://doi.org/10.1002/glia.20467.

Rau, S.W., Dubal, D.B., Böttner, M., Gerhold, L.M., Wise, P.M., 2003. Estradiol attenuates programmed cell death after stroke-like injury. J. Neurosci. 23, 11420–11426. https://doi.org/10.1523/jneurosci.23-36-11420.2003.

Robison, L.S., Gannon, O.J., Salinero, A.E., Zuloaga, K.L., 2019. Contributions of sex to cerebrovascular function and pathology. Brain Res. 1710, 43–60. https://doi.org/10.1016/j.brainres.2018.12.030.

Schindelin, J., Arganda-Carreras, I., Frise, E., Kaynig, V., Longair, M., Pietzsch, T., Preibisch, S., Rueden, C., Saalfeld, S., Schmid, B., Tinevez, J.-Y., White, D.J., Hartenstein, V., Eliceiri, K., Tomancak, P., Cardona, A., 2012. Fiji: an open-source platform for biological-image analysis. Nat. Methods 9, 676–682. https://doi.org/10.1038/nmeth.2019.

Schulz, K.M., Molenda-Figueira, H.A., Sisk, C.L., 2009. Back to the future: the organizational-activational hypothesis adapted to puberty and adolescence. Horm. Behav. 55, 597–604. https://doi.org/10.1016/j.yhbeh.2009.03.010.

Schulz, K.M., Sisk, C.L., 2016. The organizing actions of adolescent gonadal steroid hormones on brain and behavioral development. Neurosci. Biobehav. Rev. 70, 148–158. https://doi.org/10.1016/j.neubiorev.2016.07.036.

Schwarz, J.M., Sholar, P.W., Bilbo, S.D., 2012. Sex differences in microglial colonization of the developing rat brain. J. Neurochem. 120, 948–963. https://doi.org/10.1111/j.1471-4159.2011.07630.x.

Shalini, S., Dorstyn, L., Dawar, S., Kumar, S., 2015. Old, new and emerging functions of caspases. Cell Death Differ. 22, 526–539. https://doi.org/10.1038/cdd.2014.216.

Sharma, R., Mil, S. van, Melanson, B., Thomas, B.J., Rooke, J., Mallet, J.-F., Matar, C., Schwarz, J.M., Ismail, N., 2019. Programming effects of pubertal lipopolysaccharide treatment in male and female CD-1 mice. J. Immunol. 202, 2131–2140. https://doi.org/10.4049/jimmunol.1801351.

Sierra, A., Gottfried-Blackmore, A., Milner, T.A., McEwen, B.S., Bulloch, K., 2008. Steroid hormone receptor expression and function in microglia. Glia 56, 659–674. https://doi.org/10.1002/glia.20644.

Sisk, C.L., 2016. Hormone-dependent adolescent organization of socio-sexual behaviors in mammals. Curr. Opin. Neurobiol. 38, 63–68. https://doi.org/10.1016/j.conb.2016.02.004.

Sisk, C.L., Foster, D.L., 2004. The neural basis of puberty and adolescence. Nat. Neurosci. 7, 1040–1047. https://doi.org/10.1038/nn1326.

Sołtys, Z., Ziaja, M., Pawliński, R., Setkowicz, Z., Janeczko, K., 2001. Morphology of reactive microglia in the injured cerebral cortex. Fractal analysis and complementary quantitative methods. J. Neurosci. Res. 63, 90–97. https://doi.org/10.1002/1097-4547(20010101)63:1<90::AID-JNR11>3.0.CO;2-9.

Sunday, L., Tran, M.M., Krause, D.N., Duckles, S.P., 2006. Estrogen and progestagens differentially modulate vascular proinflammatory factors. Am J Physiol-endoc M 291, E261–E267. https://doi.org/10.1152/ajpendo.00550.2005.

Sweeney, M.D., Zhao, Z., Montagne, A., Nelson, A.R., Zlokovic, B.V., 2019. Blood-brain barrier: from physiology to disease and back. Physiol. Rev. 99, 21–78. https://doi.org/10.1152/physrev.00050.2017.

Tay, T.L., Savage, J.C., Hui, C.W., Bisht, K., Tremblay, M.-È., 2017. Microglia across the lifespan: from origin to function in brain development, plasticity and cognition. J. Physiol. 595, 1929–1945. https://doi.org/10.1113/JP272134.

Taylor, S.E., Morganti-Kossmann, C., Lifshitz, J., Ziebell, J.M., 2014. Rod microglia: a morphological definition. PloS One 9. https://doi.org/10.1371/journal.pone.0097096 e97096–e97096.

Varatharaj, A., Galea, I., 2017. The blood-brain barrier in systemic inflammation. Brain Behav. Immun. 60, 1–12. https://doi.org/10.1016/j.bbi.2016.03.010.

Velez-Perez, A., Holder, M.K., Fountain, S., Blaustein, J.D., 2020. Estradiol increases microglial response to lipopolysaccharide in the ventromedial hypothalamus during the peripubertal sensitive period in female mice. eNeuro 7. https://doi.org/10.1523/ENEURO.0505-19.2020. ENEURO.0505-19.2020.

Vigil, P., Orellana, R.F., Cortés, M.E., Molina, C.T., Switzer, B.E., Klaus, H., 2011. Endocrine modulation of the adolescent brain: a review. J. Pediatr. Adolesc. Gynecol. 24, 330–337. https://doi.org/10.1016/j.jpag.2011.01.061.

Villa, A., Gelosa, P., Castiglioni, L., Cimino, M., Rizzi, N., Pepe, G., Lolli, F., Marcello, E., Sironi, L., Vegeto, E., Maggi, A., 2018. Sex-specific features of microglia from adult mice. Cell Rep. 23, 3501–3511. https://doi.org/10.1016/j.celrep.2018.05.048.

Waters, E.M., Simerly, R.B., 2009. Estrogen induces caspase-dependent cell death during hypothalamic development. J. Neurosci. 29, 9714–9718. https://doi.org/10.1523/jneurosci.0135-09.2009.

Williamson, L.L., Sholar, P.W., Mistry, R.S., Smith, S.H., Bilbo, S.D., 2011. Microglia and memory: modulation by early-life infection. J. Neurosci. 31, 15511–15521. https://doi.org/10.1523/jneurosci.3688-11.2011.

Wolf, S.A., Boddeke, H.W.G.M., Kettenmann, H., 2016. Microglia in physiology and disease. Annu. Rev. Physiol. 79, 619–643. https://doi.org/10.1146/annurev-physiol-022516-034406.

Zhu, C., Wang, X., Xu, F., Bahr, B.A., Shibata, M., Uchiyama, Y., Hagberg, H., Blomgren, K., 2005. The influence of age on apoptotic and other mechanisms of cell death after cerebral hypoxia–ischemia. Cell Death Differ. 12, 162–176. https://doi.org/10.1038/sj.cdd.4401545.

Zhu, C., Xu, F., Wang, X., Shibata, M., Uchiyama, Y., Blomgren, K., Hagberg, H., 2006. Different apoptotic mechanisms are activated in male and female brains after neonatal hypoxia–ischaemia. J. Neurochem. 96, 1016–1027. https://doi.org/10.1111/j.1471-4159.2005.03639.x.